



A crustal magnetic model of Britain obtained by 3D inversion

D. Beamish^{*}, T.C. Pharaoh, D.I. Schofield

British Geological Survey, Keyworth, Nottingham NG12 5GG, UK

ARTICLE INFO

Keywords:

British tectonic terranes
Magnetic anomalies
3D inversion
Crustal scale
Subduction zone processes

ABSTRACT

The national baseline aeromagnetic survey of Britain allows a uniform assessment of the shallow and deep magnetic properties of the British tectonic terranes. The most significant is that associated with destruction of early Palaeozoic oceanic lithosphere across the Iapetus Suture separating Baltica and Avalonia from the Laurentian terranes. Here a formal 3D inversion of a continuous swathe of the data is considered. The study provides a uniform volumetric whole crust assessment extending for over 1000 km. Normally a 3D inversion of magnetic data is controlled using a variety of constraints however this is not appropriate at the crustal scale due to our increasingly imprecise knowledge of lithology at increasingly greater depths. The main crustal interface encountered occurs at the Curie isotherm depth. We demonstrate the behaviour of introducing different magnetic crustal depths and suggest the crustal 'magnetic depth' of our models can be independently constrained using global or regional studies of the deep geotherm. Static magnetic data have no inherent depth resolution. Here an empirical '1D depth' weighting and a more formal '3D distance' weighting are assessed. The inversion procedure is regularised to provide stable models appropriate to the data and their errors. To gain confidence when using such a 'geologically-unconstrained' inversion, we compare our 3D inversion results with an existing geologically-constrained 2.5D profile inversion across northern Britain. A surprising agreement in the 3D susceptibility magnitudes is observed. The chosen study area traverses 10 British terranes and images their tectonic fabric by way of non-magnetic zones (i.e. susceptibilities <0.0001 to 0.001 SI) and magnetic zones displaying geological relevance and tectonic significance at deeper crustal levels. Here we discuss the more significant 3D model features which, by virtue of a continuous crustal-scale assessment and fitting the data with a high degree of fidelity, provide additional structural insights.

1. Introduction

The remarkably varied surface geology of Britain reflects an equally varied crustal structure. The crust comprises at least 14 distinct tectonic 'terranes' with very different ages of formation, largely accreted together during the Caledonian Orogeny, ending at about 400 Ma (Fig. 1a). The Iapetus Suture Zone (Soper et al., 1992) separates the terranes of northern Britain, which have affinities with the palaeocontinent of Laurentia, from those of central and southern Britain, which have Gondwanan affinities. These two continents are inferred to have been separated by several thousand kms of Iapetus oceanic crust in mid-Ordovician time on the basis of biostratigraphic (Cocks et al., 1997; Cocks and Fortey, 1982) and palaeomagnetic (e.g. Trench and Torsvik, 1992) evidence. Significant crustal reworking and further accretion affecting southernmost Britain occurred during the Variscan Orogeny, ending at about 300 Ma.

The Laurentian terranes include crust generated in Archaean (HT

and NAT in part), Palaeoproterozoic - Mesoproterozoic (NHT, CHGT in part and ?MVT), Neoproterozoic (CHGT) and early Palaeozoic time (MVT and SUT) (Fig. 1a and Table 1). They were accreted to the Laurentian margin by early Silurian time, with late orogenic sinistral strike-slip modifying terrane boundaries and internal structure well into Devonian time (Dewey and Strachan, 2003). The Gondwana-related terranes include crust accreted to the Gondwana margin in Neoproterozoic to Cambrian (CT and NAT) and early Ordovician time (RMT), which were rifted away as a distinct 'Avalonia Composite Terrane' through later Ordovician time. Amalgamation of the Laurentian and Avalonia terranes occurred following closure of the Iapetus Ocean in early Silurian time (McKerrow et al., 1991). Opening of a contemporaneous southerly, Rheic Ocean basin, led to rifting of the Caledonian accretionary mosaic, with closure in Devonian-Carboniferous time culminating in the Variscan Orogeny. The 'Variscan Front' (VF) is the northern limit of thrust nappe displacement of the Variscan externide (Rhenohercynian) zone and is superimposed on the

^{*} Corresponding author.

E-mail addresses: dbe@bgs.ac.uk (D. Beamish), tcp@bgs.ac.uk (T.C. Pharaoh), dis@bgs.ac.uk (D.I. Schofield).

<https://doi.org/10.1016/j.tecto.2021.228982>

Received 3 March 2021; Received in revised form 8 June 2021; Accepted 23 June 2021

Available online 25 June 2021

0040-1951/© 2021 British Geological Survey, a component body of UKRI (BGS) (c) UKRI ALL RIGHTS RESERVED. Published by Elsevier B.V. This is an open

access article under the CC BY license (<http://creativecommons.org/licenses/by/4.0/>).

original Caledonian accretionary mosaic.

Fig. 1a presents a map of the inferred terranes and their boundaries (after Bluck et al., 1992; Pharaoh et al., 1996). There is ongoing debate about the significance and status of some of these elements. All the results presented here, in map and cross-section form, are referenced to this map. 14 terranes lie within the study area (460 × 1000 km); Table 1 details the codes used. Four terranes (NT, RMT, SNST and WT) lie off the transect line shown in Fig. 1 and are not discussed further in this analysis. In our central study area (Fig. 1), the Laurentian and Avalonian terranes are separated by the suture zone (ISZ) formed by closure of the Iapetus Ocean. The ISZ is concealed beneath the Carboniferous Solway-Northumberland Basin and is inferred to dip northward beneath the Southern Upland Terrane (SUT) (Soper et al., 1992). The Solway Line (SL) is the approximate surface trace of the suture as defined by Kimbell and Stone (1995). Since the 1990's, most authors (following Bluck et al., 1992) have considered the Avalon Composite Terrane, to south of the SL, to incorporate the Leinster-Lakesman Terrane (LLT), which includes the Lake District and North Pennines (Fig. 1a); the Caledonides of Southern Britain (CSB); and a nucleus of smaller terranes accreted to Gondwana in Neoproterozoic time, of which the Charnwood Terrane

Table 1

The 14 terranes that define the tectonic framework of Britain in this study. They are shown in Fig. 1. Four additional terranes shown in Fig. 1 (NT, RMT, SNST and WT) denoted with an asterisk, lie largely outside the main study area and are not discussed here.

Label	Terrane	Age of crustal formation
CHGT	Central Highlands Grampian Terrane	Proterozoic
CSB	Caledonides of Southern Britain	Neoproterozoic
CT	Charnwood Terrane	Neoproterozoic
HT	Hebridean Terrane	Archaean
LLT	Leinster-Lakesman Terrane	Ordovician
MVT	Midland Valley Terrane	?Mesoproterozoic
NAT	North Armorican Composite Terrane (east)	Archaean-Proterozoic
NHT	Northern Highlands Terrane	Archaean
RMT*	Normannian Terrane	Neoproterozoic
RMT*	Rosslare-Monian Terranes	Neoproterozoic
SNST*	Southern North Sea Terrane	?Ordovician
SUT	Southern Uplands Terrane	Ordovician
VRZ	Variscide Rheohercynian Zone	Neoproterozoic
WT*	Wrekin Terrane	Neoproterozoic

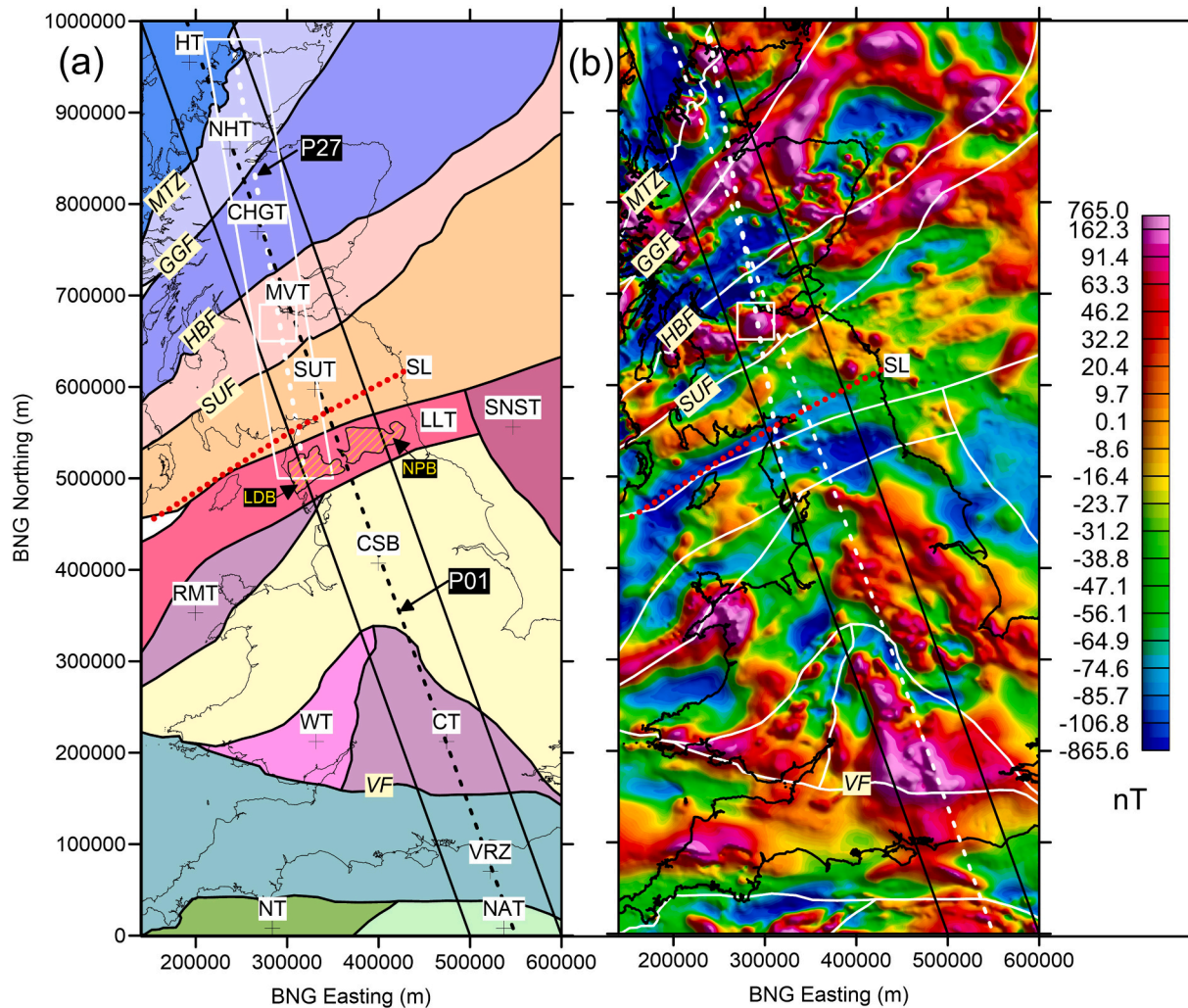


Fig. 1. The study area and magnetic anomaly (TMI) data across Britain. Both panels show the NNW swathe selected for 3D magnetic inversion (solid black lines). The central dash line (Profile P01, 1062.8 km long) is used for cross-sections. (a) tectonic terranes (see Table 1) with 3 boundaries identified as MTZ (Moine Thrust Zone), GGF (Great Glen Fault), HBF (Highland Boundary Fault). VF is the Variscan Front. SL is the Solway Line. A second polygon in the north (white line boundary) forms a more detailed study area for comparison with an existing profile model. The central white dash line within this polygon identifies profile P27. A 40 × 40 km square in the Midland Valley Terrane (MVT) is centred on the Bathgate anomaly. Two polygons (with cross-hatch) in Leinster-Lakesman Terrane (LLT) outline granite batholiths: LDB (Lake District Batholith) and concealed NPB (North Pennine Batholith). (b) the magnetic (TMI) data upward continued to a height of 2 km. Equal area colour plot. BNG refers to British National Grid coordinates which are used throughout this study.

(CT) is one example (e.g. Pharaoh and Carney, 2000). There is no faunal evidence to suspect that these terrane elements were significantly separated during Ordovician time. Indeed, following accretion of RMT to the Gondwana margin in early Ordovician time (Schofield et al., 2020), the CSB and LLT comprise sedimentary and volcanic domains subsequently deposited/accreted at the edge of Avalonia following rifting of the latter from the Gondwana margin. In CSB the Caledonian basement is largely concealed by later strata and potential field data have been used to identify some of the broad structural trends (Lee et al., 1990; Pharaoh et al., 1995). Irrespective of whether these elements constitute terranes or domains, the familiar nomenclature is retained here to facilitate their location and description in the text.

The purpose of the present study is to use existing aeromagnetic baseline data (Fig. 1b) to quantify the crustal scale magnetic structures associated with each of the complex set of assembled terranes. By definition, each of the terranes has a separate and distinct geological history that preceded the present accreted assemblage. The country-wide aeromagnetic data, used here, are vintage (low resolution) and can only accommodate a grid sampling of no better than 500 m (with some areas requiring interpolation). A previous paper (Beamish et al., 2016), using a much larger baseline data set, mapped the deep (lower crustal) magnetic bodies responsible for the longest wavelength features. The main analysis employed spectral decomposition of the data and an approximate but widely used edge-detection procedure (the tilt derivative).

The present study is undertaken using 3D magnetic inversion which provides continuous subsurface estimates of magnetic susceptibility using rectilinear voxels. As indicated in Fig. 1b, only a central subset of the complete data coverage is used in the inversions. The use of such a swathe reduces the computational resources required and still achieves an adequate crustal scale assessment of the terranes encountered. Our main purpose is to demonstrate the procedures that can be applied, universally, to very large scale, country-wide aeromagnetic data sets. In our case, the central profile P01 (Fig. 1) is over 1000 km in length. Although 3D inversion procedures have been available for some time they have rarely been applied at the crustal scale. The most informative inversion results are obtained when the model can be constrained by structural, geological or other existing information. Such constraints are rarely precise (i.e. without uncertainty) and they are not available at the crustal scale without speculation. In order to gain confidence when using such a 'geologically-unconstrained' inversion, we compare our 3D results with an existing geologically-constrained 2.5D inversion along profile P27 shown in Fig. 1. This is the North Britain profile presented by Rollin (2009) and is 486 km in length. It is well known that static magnetic data have no inherent depth resolution and numerical strategies for dealing with this are required. Here an empirical '1D depth' weighting and a more formal '3D distance' weighting are assessed and used. The inversion procedure is regularised to provide stable, but smooth models appropriate to the data and their errors. Apart from the crustal magnetic depth, the inversion procedure is otherwise unconstrained. Similar unconstrained crustal scale 3D inversions are presented by Goodwin et al. (2015).

When dealing with a crustal scale magnetic model, the base of the model considered will be physically determined by the Curie depth. This depth (the Curie-temperature isotherm) corresponds to the temperature at which magnetic minerals lose their ferromagnetism. We concur with Frost and Shive (1986) and Kimbell and Stone (1995) that magnetite is the main magnetic mineral in the lower crust and thus assume 580 °C to be the Curie temperature. Magnetic minerals at greater temperatures are paramagnetic and, from the perspective of the earth's surface, are essentially nonmagnetic. Thus, the Curie-temperature isotherm corresponds to the basal surface of any magnetic crustal model. Recently the Curie depth across Britain has been assessed by Baykiev et al. (2018) under the assumptions discussed above. The authors studied the lithospheric structure of the British Isles using a methodology that allows for forward modelling of the Curie temperature depth based on seismic,

elevation and gravity observations within an integrated geophysical-petrological approach (LitMod3D). The lithospheric geotherm is computed in 3D under the assumption of steady-state heat conduction. Additionally a new seismically constrained Moho depth map was generated. Across onshore Britain the Curie depth contours (Baykiev et al., 2018, Fig. 9B) range from 27.5 km (western Scotland) to 32.5 km (Southern England). Between these limiting values, the predominant depth is around 30 km. The results also indicate that across onshore Britain the Curie depth lies above the seismic Moho. Although we have experimented with different magnetic crustal depths (discussed later) our main inversion results use a 'maximum' crustal magnetic depth of 32 km. Horizontal interfaces in susceptibility do not produce a magnetic anomaly. The inversion procedure, by itself, is thus unable to establish the crustal magnetic depth and this must be supplied as an independent constraint.

Depth slices and cross-sections are extracted from the 3D model volume (comprising 2x2x2 km voxels) in order to compare the susceptibility distribution obtained with existing (non-3D) knowledge. The inversion models image the compartmentalisation of the crust into non-magnetic zones (i.e. susceptibilities <0.0001 to 0.001 SI) and magnetic zones displaying geological and tectonic significance. Depth slices necessarily reflect the lateral characteristics observed in the data themselves. Crustal scale cross-sections also offer a valuable summary of the magnetic structure of the UK crust. Since the inversion produces inherently smooth models, we demonstrate the use of 3D volumetric gradients to aid interpretation. The magnetic features across Britain have been studied and reported on for many decades. To a large extent the existing studies provide modelling and interpretations of the magnetic features also encountered in our 3D model. Our discussion is therefore limited to the more significant 3D features which, by virtue of a continuous and crustal-scale assessment, provide additional structural insights into the magnetic fabric of the assembled terranes.

2. Materials and methods

2.1. The data

The magnetic data used here have been described many times previously (Busby et al., 2006; Kimbell et al., 2006; Rollin, 2009). The baseline aeromagnetic data for the UK (largely onshore) were acquired between 1955 and 1965. The flying height was about 305 m and flight line spacing was typically 2 km. A subset of the baseline TMI (Total Magnetic Intensity) data, comprising a NW-SE swathe used for the 3D inversion is identified in Fig. 1b, within the wider rectilinear data set. The lateral Easting extent of the central transect (P01) is 100 km (greater than 3 crustal scale lengths).

The purpose of using a 'reduced scale' swathe as opposed to a full rectilinear analysis is simply to accommodate the many inversion experiments that are necessary using only modest computer resources. The same principle can be applied to many more newly-acquired, country-wide aeromagnetic data sets to obtain continuous crustal scale assessments across tectonic assemblages. The swathe can be linear, as here, or dogleg to accommodate variations in spatial trends. It should be noted that modern survey data may provide high spatial sampling (50 to 100 m in grid form). Here we assess how a reduced resolution of 1 or 2 km (data down-sampling) can provide an adequate gross crustal assessment across large scale data sets. The central axis of the swathe (profile P01) is used to extract and present crustal susceptibility cross-sections across the terranes.

The typical maximum grid resolution that can be obtained using the UK baseline data is 500 × 500 m. Here, again to accommodate modest resources and to provide a degree of smoothing, we employ a grid cell size of 2 × 2 km. The appropriate voxel lateral scale length of our models is then also 2 × 2 km. It is common practice to upward continue the data to an elevation that is commensurate with the voxel scale length used (Li and Oldenburg, 1996; Goodwin et al., 2015). Here we upward continue

the data to a height of 2 km (i.e. 305 + 1695 m) and these are the data shown in Fig. 1b. The data across central profile P01 are shown in Fig. 2a. It can be seen that the largest peak-to-peak anomaly excursion is associated with the Great Glen Fault (GGF). Both original and upward continued (UPC) data are shown. The upward continuation by 1695 m results in a significant smoothing. The smoothing is quantified in Fig. 2c which shows the difference in the two data sets. The high wavenumber contributions that are omitted in the upward continued data are particularly intense across the three northern-most terranes, only modest differences occur across the SUT and LLT terranes. The behaviour identified in Fig. 2 represents the higher wavenumber structural contributions that would not be resolved in an inversion using voxel scale lengths of 2 km. Normally, when inverting for upper crustal or 'local' anomalies, a regional trend is removed from the data (e.g. Andersson and Malehmir, 2018). This ensures that the regional features do not adversely influence the local model; here we necessarily use the full wavenumber content of the data.

2.2. 3D magnetic inversion

The inversion method used here was originally developed by Li and Oldenburg (1996) and is referred to as MAG3D. The literature largely contains examples in the use of the algorithm for near surface mineral exploration where additional observations (e.g. borehole measurements

of susceptibility) provide constraints across an exploration play. Li and Oldenburg (1996) note however that the method is general and applicable to problems at all scales. It is undoubtedly true that the most informative results are obtained when the model can be constrained by structural, geological or existing information e.g. on the true range of susceptibilities over a given depth interval (e.g. Spicer et al., 2011). While this type of information might be obtained and used in the near-surface, the procedure of attempting to constrain most aspects of a large scale, crustal inversion would be largely speculative and the degree of speculation would increase with increasing depth. In the absence of such constraints, as at the crustal scale here considered, the procedure is referred to as a geologically-unconstrained inversion (Lelièvre et al., 2009). Since no constraints are applied (other than magnetic crustal depth), the model produced might be considered 'non-geological'. In order to assess the geological significance of the model(s), the unconstrained inversion results are later compared with existing, highly constrained results from 2.5D modelling across a 487 km profile (Profile P27, Fig. 1).

The MAG3D algorithm assumes that the measured magnetic field is produced only by induced magnetization and a positivity constraint is usually applied to the susceptibility. Here we use a positivity constraint and unconstrained susceptibility amplitudes throughout. The subsurface distribution is represented by a large number of rectilinear cells (voxels) of constant susceptibility, and the final solution is obtained by finding a

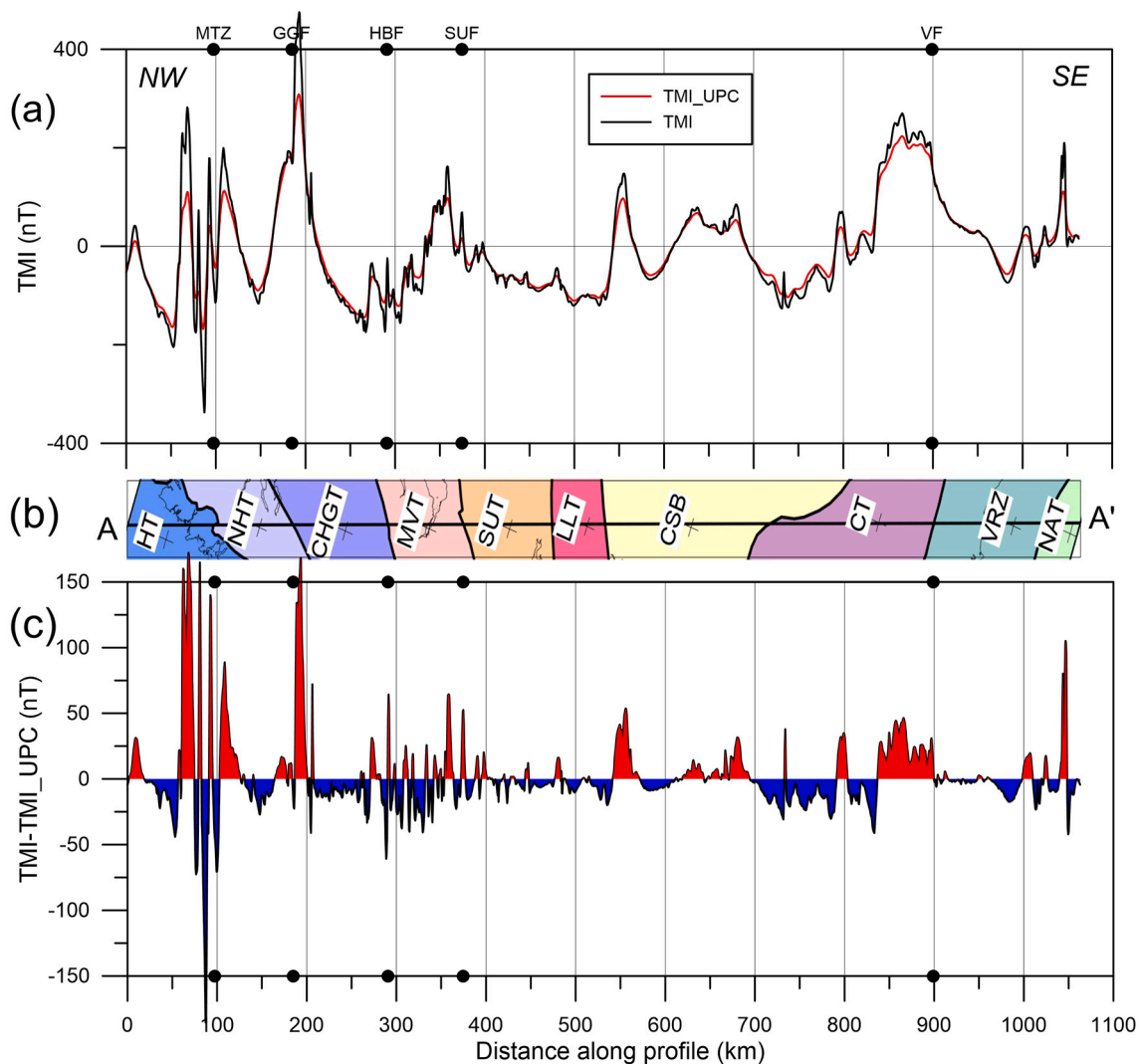


Fig. 2. TMI data along profile P01. (a) Observed and upward continued (UPC) data (to a height of 2 km). (b) Terranes along central profile P01 (see Fig. 1 and Table 1). (c) Difference between observed (nominal height of 305 m) and upward continued data.

model that reproduces the data adequately and at the same time minimizes a model objective function penalizing the structural complexity of the model (using a reference model and smoothness constraints).

In the case of a zero-valued reference model, as used here, the inversion is encouraged to recover models with low values of susceptibility. The model returned then provides the simplest distribution of non-magnetic material (and *ipso facto*, magnetic material) consistent with the observations. The objective function contains a term defining *smallness* and 3 terms defining directionally dependent smoothing scale lengths which can generate a range of model types. The first of the four components of this equation measures the smallness (difference) between the reference and the recovered model. The smoothing lengths define how smoothly the recovered model cell properties vary between adjacent voxels in each direction.

The appropriate parameters (smallness and scale lengths) assigned require careful experimentation. Ideally for a structural investigation, the degree of smoothing applied should be minimised so that boundaries in susceptibility are better resolved. The approach adopted here was to start with a minimum amount of smoothing and to increase the degree of smoothing while examining the total spatial gradient:

$$\|\nabla m\| = \sqrt{(\nabla_x m)^2 + (\nabla_y m)^2 + (\nabla_z m)^2} \quad (1)$$

(Lelièvre et al., 2009) across each recovered voxel model. As expected, instabilities in the spatial gradient (model noise) were found to decrease with amount of smoothing. For this data set and using uniform voxels of $2 \times 2 \times 2$ km, a low degree of smoothing that equates to smoothing across distance scales of $4 \times 4 \times 4$ km was employed when necessary.

Estimated noise levels (standard deviations) for the data must be assigned to provide a global target misfit for the inversion. As noted by Williams (2008) there is no perfect guideline for assigning the correct level of uncertainty in any data set but suggests a 5% level when magnetic data, with a high dynamic range, are to be inverted. In broad terms, a high standard deviation will result in more simplified outcomes while standard deviations that are too low run the risk of providing solutions of a non-geologic form. The appropriate choice must be made by experimentation with the data set under consideration. For our data, upward-continued to a height of 2 km (Fig. 2), we found, surprisingly, that a fixed base level standard deviation of 2 nT provided relatively stable inversion results. Noise was apparent only when spatial derivatives were calculated across these models; it was then necessary to increase the standard deviation to 3% of each data value and include the 2 nT base level. It should be noted that large numbers of models were assessed in this study before a set of final, preferred models were chosen.

2.3. Incorporation of depth: Depth and distance weighting

Potential field data contain no inherent information on the depth of the causative bodies. A crucial aspect of the inversion is therefore the incorporation of depth, or distance, weighting. The weighting function is designed to counteract the $1/r^3$ decay of the magnetic field response (of a cubic cell) with distance from the source so that all cells have an equal likelihood of containing sources. No weighting would result in a model with sources clustered near the surface where the data has the most sensitivity. The weighting function has two possible forms referred to as depth and distance weighting (Li and Oldenburg, 1996). Depth weighting is applied only to the column of voxels beneath each observation point. Distance weighting is more general and allows for the true 3D separation of observations and cells (i.e. lateral as well as vertical separations). Li and Oldenburg (1996) indicate that when these weightings are used, the susceptibility model constructed by minimizing the model objective function, subject to fitting the data, places the recovered anomaly at approximately the correct depth.

The literature appears to lack comparisons of the two weighting methods applied to specific data sets. When, as here, the data are uniformly sampled (from gridded data) it is possible to directly compare the

results obtained. The use of uniform ($2 \times 2 \times 2$ km) voxels across the model mesh also approximate spheres which directly conform to the $1/r^3$ decay of magnetic field anomalies. We choose the results obtained with a 40 km crustal magnetic model. Although this is an excessive depth, it is chosen to allow later comparisons with more realistic crustal magnetic depths.

The core area model, as defined in Fig. 1, contains $230 \times 500 \times 20$ cells and is covered by 25,149 observations. The two inversions, shown in Fig. 3, both use an assumed 2 nT error floor and susceptibility amplitudes were unconstrained. The two inversion results both provide a misfit standard deviation of just less than 2 nT and so both solutions are equivalent. The two susceptibility cross sections, extracted from the 3D inversion, along the profile P01 are shown in Fig. 3. The cross-sections use a vertical exaggeration of $\times 5$ which means, for example, that a true structural dip of 45° is translated to an apparent near-vertical dip of $\sim 79^\circ$. The susceptibilities along the profile display a series of higher value zones that show a degree of correspondence with the identified tectonic zone interfaces (faults and terrane boundaries) from Fig. 1. Much of the crustal volume is also associated with low or 'non-detectable' values of susceptibility (values less than say 0.001 SI). When the two cross sections are compared it is clear that there is a high degree of correspondence in the lateral and vertical 'boundaries and zones' of the higher susceptibility regions identified. A single contour value of 0.1 SI is used to aid the comparison. The depth weighting solution provides some higher value zones than its distance weighting counterpart (largely confined to the upper 30 km). The general form of the susceptibility distribution obtained by both, equally acceptable, solutions is repeated in all the subsequent inversions discussed here. The models obtained represent the simplest distribution of detectable magnetised zones (bodies) that are superimposed on a reference crustal model of zero susceptibility.

2.4. Crustal model depths

It was previously noted that the inversion procedure, by itself, is unable to establish the crustal magnetic depth and this is best supplied as an independent constraint. A series of inversions were carried out using depth weighting and a target misfit of 2 nT. It was found that adequate misfits, and hence models, could be obtained by assigning crustal magnetic depths of between 5 and 40 km. The number of data used throughout is 25,149 and the models obtained have chi-square misfits of between 24,869 and 25,170 with associated standard deviations of between 1.92 and 1.98 nT.

The inversion largely adjusts the vertical distribution of susceptibilities to accommodate the different maximum depths assigned. This is illustrated in Fig. 4 which compares the models obtained along profile P01 using a 20 km crustal depth (Fig. 4a) and a 30 km crustal depth (Fig. 4b). A 20 km crustal depth is significantly underestimated while the 30 km depth should be approximately correct. Fig. 4c is the difference in the 2 models (a-b) to a depth of 20 km. Increases in susceptibility are shown using the same colour scale as the models (a) and (b) while the much less significant decreases in susceptibility are shown as an entirely white zone. It is evident that more localised bodies restricted to the upper crust (0–10 km) are largely unchanged in the 2 inversions but that the 20 km crustal model would require enhanced susceptibilities throughout its lower part to achieve the required misfit. It should also be noted that the lateral distribution of susceptibility remains largely unchanged and the major adjustments are made to the vertical stack of voxels beneath each observation point. Similar behaviour arises in the case of 3D gravity inversion as discussed by Welford and Hall (2007).

To complete the analysis the data misfit (observed minus predicted values) along the profile for both 20 km and 30 km crustal magnetic depths are shown in Fig. 5. Over the majority of the profile both models return very similar misfits well within the specified ± 2 nT error limit. The largest and most persistent misfits occur in the vicinity of the Moine Thrust Zone (MTZ) and the 2 km data sampling may be inadequate to

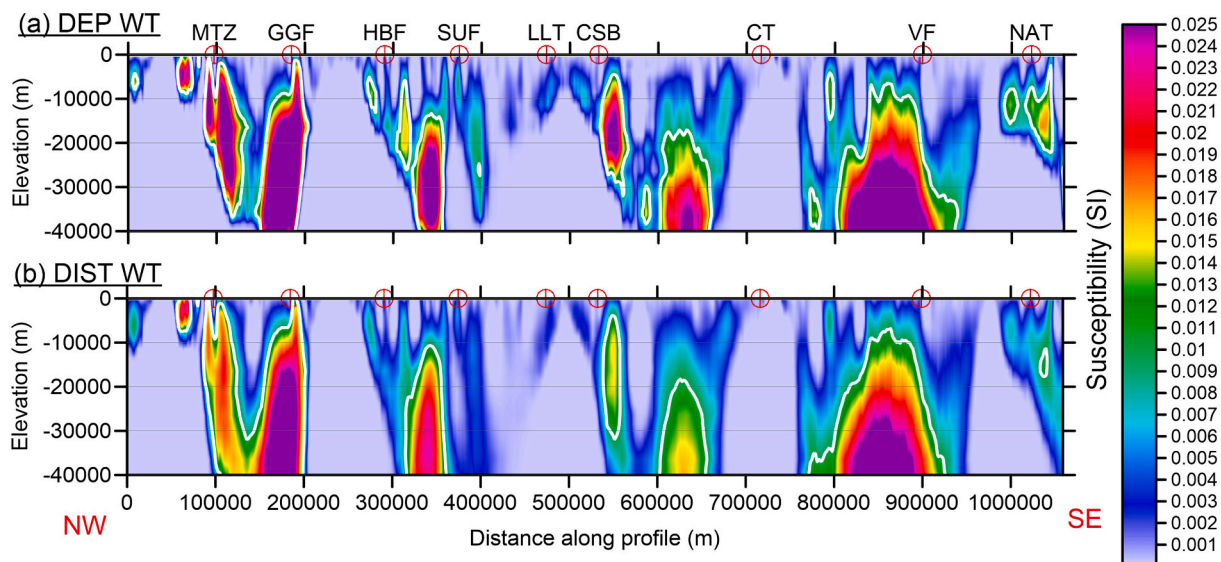


Fig. 3. 3D inversion cross-section results along profile P01 used to illustrate the influence of 2 weighting procedures. (a) Results using a depth weighting scheme and (b) results using a distance weighting scheme. Both inversions assume a crustal magnetic depth of 40 km. The white contour denotes a value of 0.01 SI. Cross-hair symbols with labels denote location of terrane boundaries (Fig. 1 and Table 1) along the profile and additionally the Variscan Front.

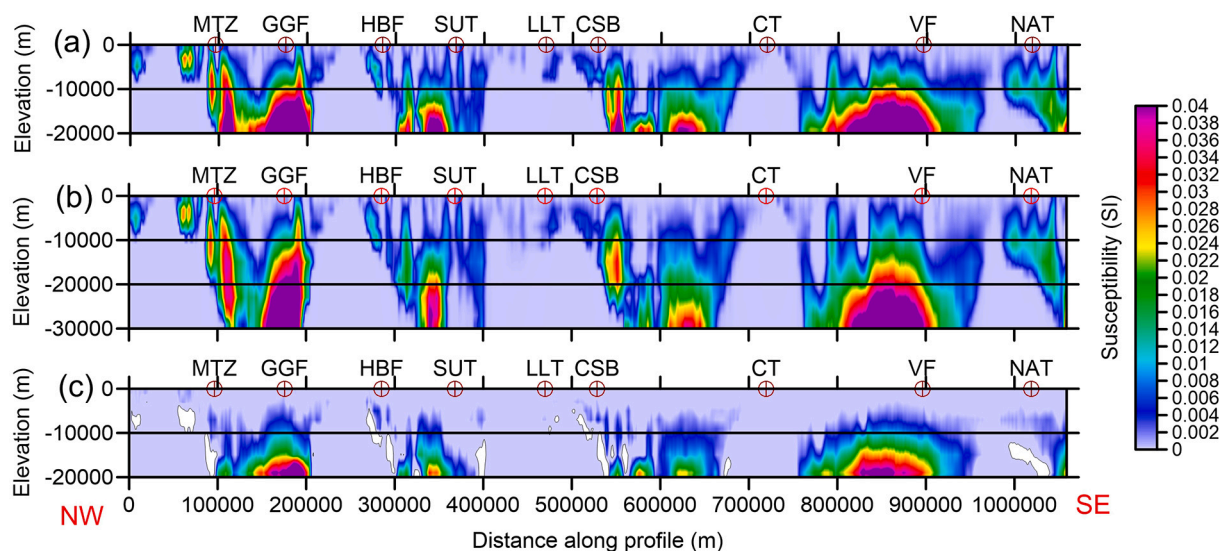


Fig. 4. 3D inversion cross-section results along profile P01 used to illustrate the influence of the crustal magnetic depth. Cross-hair symbols with labels denote location of terrane boundaries (Fig. 1 and Table 1) along the profile and additionally the Variscan Front. (a) 20 km depth and (b) 30 km depth. (c) is the difference (a) minus (b) to the same depth of 20 km. The observed increases in the susceptibility difference use the same colour scale as the cross-sections. Decreases in susceptibility are shown as white zones.

capture the complex gradients observed here (see Fig. 2). Additionally, a long wavelength misfit occurs to the north of the Highland Boundary Fault (onset at ~ 250 km) which differs in the 2 models amounting to 5 nT in the more realistic 30 km crustal model.

2.5. Comparison of unconstrained 3D inversion and existing geologically-constrained 2.5D inversion

We now compare existing crustal magnetic modelling with the results obtained by 3D inversion. The main method of characterising the magnetic character of the deeper crust across Britain has largely been through 2.5D profile modelling. The modelling has used both magnetic and gravity anomaly variations (separately) alongside structural information provided by outcrop mapping and (where available) results from boreholes and seismic surveys. The joint modelling of magnetic and

gravity variations is then further controlled by judgements of the geological-tectonic (i.e. 'terrane') framework along the profile. This understanding guides the geometries of the polygons used to juxtapose geophysical properties. The methods have been widely and jointly applied to the aeromagnetic data (used here) and land-based gravity data within 3 large and overlapping regional areas of South East England, Southern Scotland & Northern England and Northern Scotland (Busby et al., 2006; Kimbell et al., 2006; Rollin, 2009, respectively). In the published models, geological units are represented by polygons which are assumed to be traversed orthogonally by the selected model profile. The polygons extend symmetrically (and with constant cross-section) to each side of the profile by a distance that can be defined by the interpreter.

The models are by no means unique as it is possible to reproduce a given anomaly by a variety of property distributions. Two strategies help

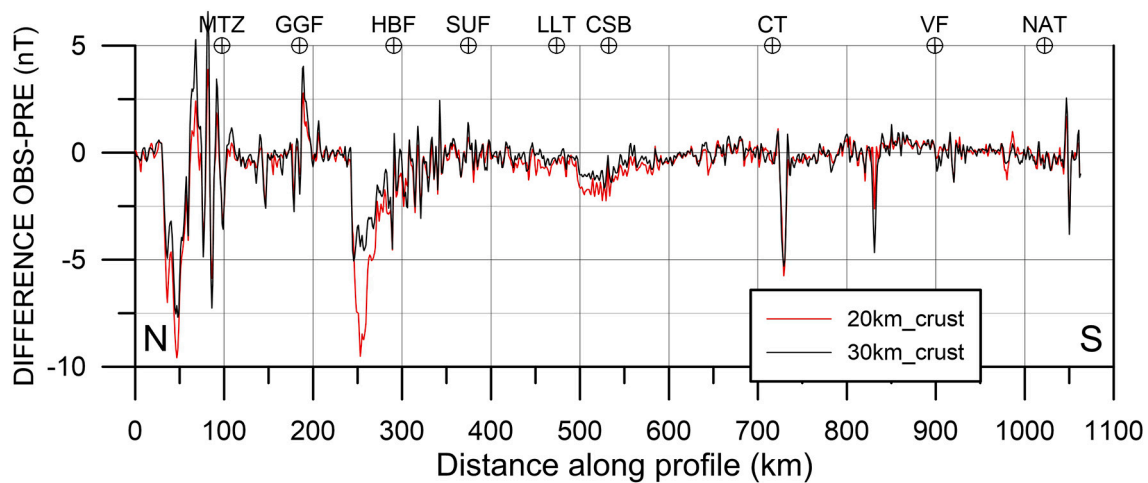


Fig. 5. Difference between observed (OBS) and modelled/predicted (PRE) data of the 20 km and 30 km magnetic crustal depth models shown in Fig. 4, along profile P01. The target misfit was specified as ± 2 nT. Cross-hair symbols with labels denote location of terrane boundaries (Fig. 1 and Table 1) along the profile and additionally the Variscan Front.

to reduce the uncertainty. Firstly, the properties assumed for the components of the models are guided by field and laboratory measurements of rock densities and magnetic properties. Secondly, the geometry of these units is constrained by data available from other sources, in particular geological mapping and seismic surveys. The BGS geological map series at 1:250,000 scale was the primary source of information on the locations of exposed geological units and boundaries. Even with these constraints, there is considerable latitude in the way the source of a given geophysical anomaly can be simulated. Short-wavelength anomalies are constrained to be generated by features at relatively shallow depth, but longer wavelength anomalies can be explained by a deep, sharp contrast or by a more gradual change at a shallower level.

Profile P27 (Fig. 1) was the longest of a large number of cross sections considered by Rollin (2009) across northern Britain. The profile is referred to as The North Britain profile and spans the study area from the Leinster-Lakesman Terrane (LLT) in the south through to the Northern Highland Terrane (NHT). It was sited to avoid most of the voluminous late tectonic Caledonian granites (discussed later). The main large scale

magnetic feature, and centred on the profile, is the Bathgate anomaly (Fig. 1). The magnetic data from the profile study are shown in Fig. 6a. The assemblage of polygons used for the joint magnetic and gravity modelling are shown in Fig. 6b.

The polygons constitute an initial informed geological model. The geological model (not shown here) extends to a depth of 40 km and contains 33 classifications. The magnetic model used however is effectively a 20 km crustal model. Fig. 6b shows the final model susceptibilities that provide the calculated data that are compared with the observed data in Fig. 6a. Lower crustal (20–30 km) susceptibilities were assigned a zero value. It can be noted that only a portion of the geological polygons (17) have been assigned non-zero susceptibilities to obtain the calculated fit to the data. The largest susceptibilities (0.035 SI) were assigned to the magnetic rocks beneath the Midland Valley (Bathgate anomaly). Equally, the densities assigned in the gravity modelling (not discussed here) are predominantly close to a value of 2.75 Mg.m^{-3} (the Bouguer reduction density), with the majority of significant departures confined to basins in the uppermost 2 km.

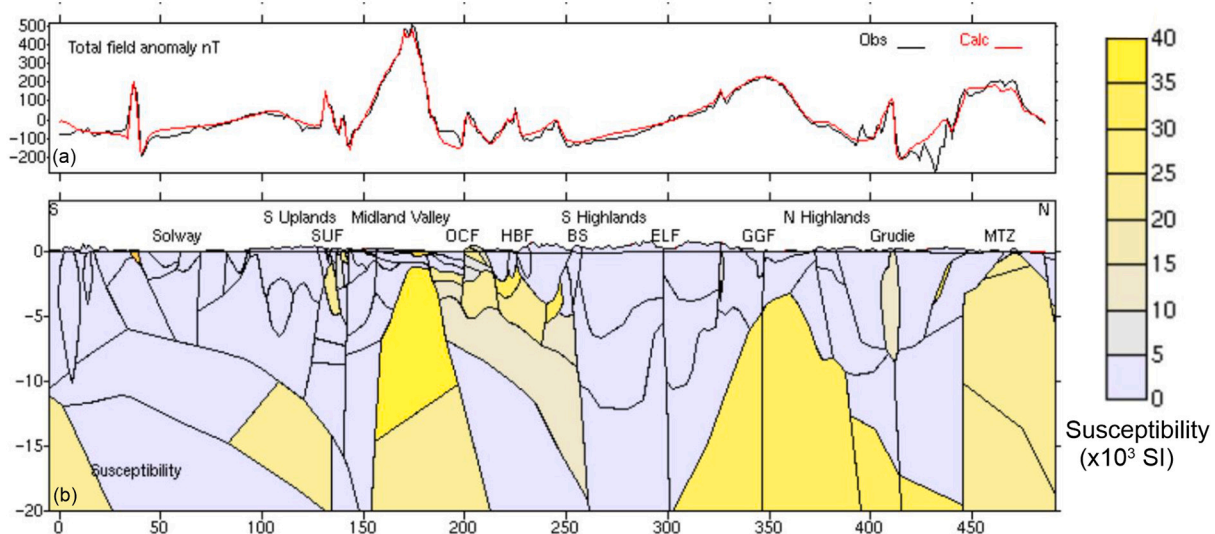


Fig. 6. Published magnetic model along Northern Britain profile P27 after Rollin (2009). (a) Data (observed in black and calculated in red) along profile P27 from South to North. (b) 2.5D susceptibility model along profile producing calculated data. Solway = Solway Basin, SUF=Southern Upland Fault, OCF=Ochil Fault, HBF=Highland Boundary Fault, BS=Boundary Slide, ELF = Ericht-Laidon Fault, GGF = Great Glen Fault, Grudie = Grudie granite, MTZ = Moine Thrust Zone. (For interpretation of the references to colour in this figure legend, the reader is referred to the web version of this article.)

In order to better compare the existing 2.5D magnetic model with that obtained by a 3D inversion we undertook an inversion using a data sampling and voxel dimension of 1 km. The swathe of data selected to model profile P27 is shown in Fig. 7a along with terrane and fault boundaries. The width of the swathe is 60 km i.e. about a crustal scale length on either side of the central profile. Many off-profile influences on a 2D profile assessment, across a crustal scale, can be noted. The profile intersects the Bathgate anomaly centrally but traverses a saddle point across the large anomaly associated with the GGF.

As discussed previously, the data were upward continued to a 1 km (305 + 695 m) level prior to inversion (to stabilise the procedure). This level of upward continuation is appropriate for the data and voxel scale of 1 km. The upward continued data extracted along P27 are shown in Fig. 7b alongside the original data. The latter replicate the data that would have been used by Rollin (2009) and are shown in Fig. 7a. It can be seen that only a slight reduction in high wavenumber content has been introduced by upward continuation.

The inversion model was constructed using $1 \times 1 \times 1$ km voxels extending to a depth of 20 km. We discuss the equivalent 3D model extending to a depth of 32 km later in the study. The core area model contains $138 \times 480 \times 20$ cells and is covered by 28,597 observations. Results using a depth weighted inversion scheme with no spatial smoothing are presented here. An assumed 2nT error floor was assigned to the data and susceptibility amplitudes were unconstrained. The inversion model provided a misfit standard deviation of just less than 2 nT with a maximum-minimum range from 17 to -44 nT across the entire area. The misfit (observed minus predicted values) along profile P27 is shown in Fig. 8. The predicted data fit the observations with a high degree of fidelity at all wavelengths. This is in direct contrast to the existing 2.5D model (Fig. 6a) in which the misfit achieved by the model can exceed 100 nT.

A cross-section of the 3D model along profile P27 is shown in Fig. 9 below the published 2.5D model (from Fig. 6). The cross-sections use a vertical exaggeration of $\times 6.52$ which means that a true structural dip of 45° would be translated to an apparent near-vertical dip of $\sim 81^\circ$. The

existing model uses discrete ‘polygon’ values of susceptibility while the 3D model distribution is continuous and smooth. Fig. 9b displays the 3D cross-section using contour intervals/colours that replicate the published results of Fig. 9a. The comparison indicates that the broad amplitude levels returned by the inversion are consistent with those of the 2.5D model. This result is significant in that the amplitude levels within the 3D inversion were totally unconstrained. It is also evident that the broad zones of both zero (non-magnetic) and high susceptibility are largely replicated in the 3D inversion model. Detailed differences can be noted and these are better assessed using the continuous colour scale in Fig. 9c. This demonstrates a much more detailed set of low contrast (<0.005 SI) features in the upper crust (0–5 km) which result from accurately fitting the high wavenumber content of the data (see Fig. 8). The misfit of the 2.5D model has to be inferred from Fig. 6a. It is evident that the fit achieved by the 2.5D model is spatially variable and significant misfit differences are apparent ranging from tens to well over 100 nT.

We first note 2 granite-classified polygons labelled A and E in Fig. 9a. Granite A is associated with the underlying Lake District Batholith (discussed later) towards the origin of the profile. This granite was assigned a zero susceptibility in the 2.5D model but is clearly imaged in the 3D model. The northern Grudie granite, labelled E, is equivalently imaged in both models. A strong isolated response occurs at around 30–40 km along profile (Fig. 7) in association with the southern-most terrane boundary. In the 2.5D model the response is modelled by a single at-surface polygon (labelled B) extending to about 1 km. The lithology (Eycott Volcanic Group) is described as basalt-spilite and has an assigned high susceptibility of 0.028 SI. In the 3D model, when the shoulders of the response are accurately modelled an at-surface, but much deeper anomaly, is imaged. This deeper anomaly is more in keeping with the 2.5D modelling of the exposed Eycott Volcanic Group undertaken by Kimbell et al. (2006) which included a significant remanent component of magnetisation. Their model (along their Profile 2) shows highly magnetic zones extending to depths just in excess of 5 km.

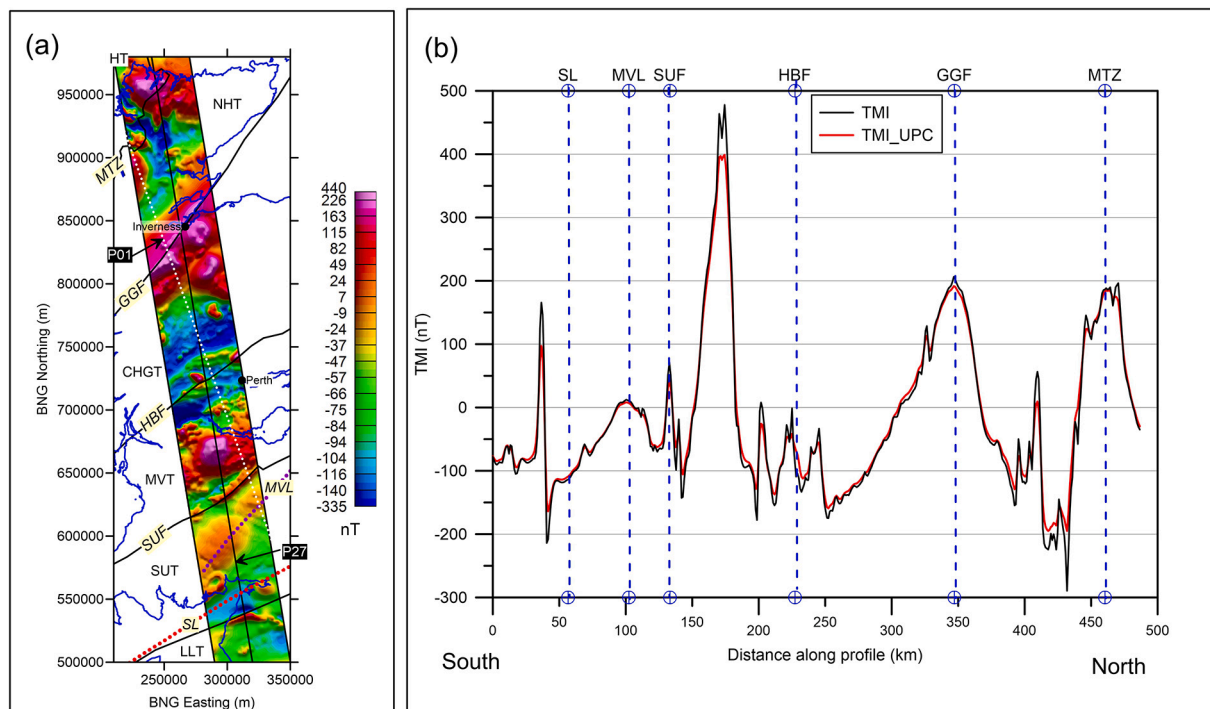


Fig. 7. Data used in 3D inversion of Northern Britain profile P27. (a) Equal area colour image of data within the inversion polygon, showing location of terranes and terrane boundaries (Fig. 1 and Table 1) along the profile. Additional boundaries are MVL: Moffat Valley Lineament and SL: Solway Line. Centre line of polygon is profile P27. (b) Observed TMI data and upward-continued data (UP_C), to a height of 1 km, along profile P27.

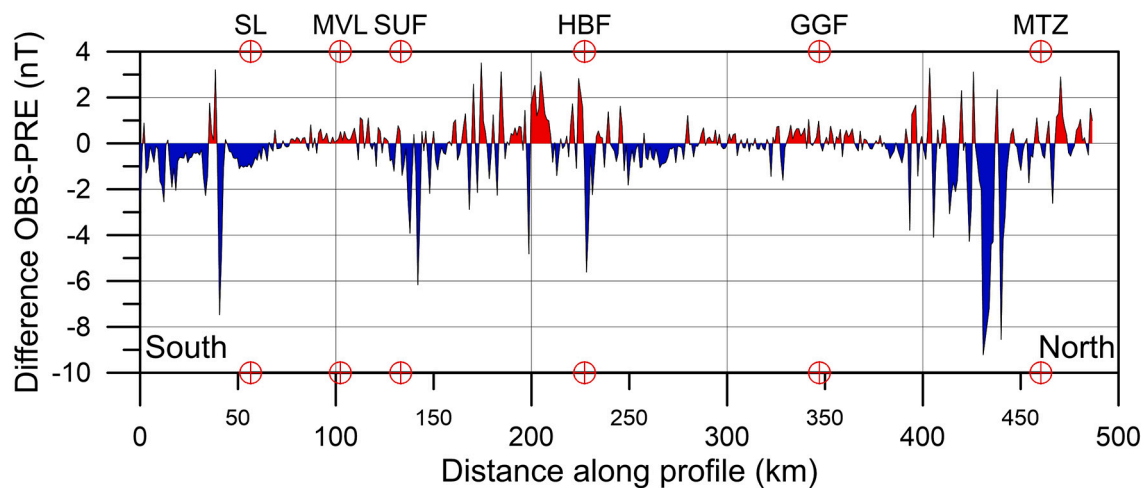


Fig. 8. Difference between observed (OBS) and modelled/predicted (PRE) data along Northern Britain profile P27. The target misfit was specified as ± 2 nT. Cross-hair symbols with labels denote location of terrane boundaries (Fig. 1 and Table 1) along the profile. Additional boundaries are MVL: Moffat Valley Lineament and SL: Solway Line.

In Fig. 9a, the mid-crustal layer beneath the Southern Uplands (labelled C1, C2, C3) includes magnetic units which, according to Rollin (2009) may be subducted volcanic arcs or microcontinental fragments (Kimbell and Stone, 1995; Kimbell et al., 2006). Only one of the polygons (C2) has a non-zero (~ 0.2 SI) susceptibility. The 3D model also images a magnetic zone underlying the SUT with a distinctly different geometry but again possessing a northward component of dip and terminating at a depth of 15–20 km just south of the Southern Upland Fault (SUF). The position of the Moffat Valley Lineament (MVL), marking an important discontinuity in geochemical data (Stone et al., 1993; Kimbell and Stone, 1995), is shown for reference.

Both models also require an isolated and laterally compact magnetic zone in association with the SUF. This zone potentially comprises ophiolitic rocks similar to those exposed in the Ballantrae Complex to the south west (Kimbell et al., 2006). As in the 2.5D model, the highest sustained susceptibilities of the 3D model are associated with the crustal scale Bathgate anomaly and the 3D model result is commensurate with that of the 2.5D model. Probably the largest ‘geometrical’ difference between the 2 models occurs north of the Bathgate anomaly and the Highland Boundary Fault (HBF). Here the MVT is shown extending at depth (polygon D, Fig. 9a) north of the HBF approximately as far as the Boundary Slide (BS). The latter is a high strain zone now termed the Grampian–Appin group junction according to Stephenson et al. (2013). The 3D model images separate anomalies largely confined to the upper crust (< 10 km) but again terminating at the Boundary Slide. The specific behaviour of the 3D model in this region is discussed in more detail later. Profile P27 traverses a saddle point in the magnetic response across the Great Glen Fault (GGF) (Fig. 7a). The broad features of the fault zone appear commensurate in both models with the 3D model showing a set of detailed features that cannot be accommodated by the 2 large polygons of the 2.5D model. In the vicinity of the northern Moine Thrust Zone (MTZ) the anomaly pattern is complex and three dimensional (Fig. 7a) and the profile crosses the surface trace twice (not acknowledged in the published model shown in Fig. 7a). Both models identify a high susceptibility zone with an upper crustal edge at around 450 km. The 3D model however images a complex whole crustal zone with a strong component of dip to the north. In true scale, although the zone is arcuate, the broad dip angle is about 30° .

In summary the comparison conducted indicates that if the 2.5D model is considered geologically/tectonically plausible then the 3D model should be considered equally plausible. A remarkable high degree of correspondence in susceptibility amplitudes is demonstrated. The inversion model allows for 3D contributions to the response, makes no

geological assumptions and reproduces the observed data with a high degree of precision.

3. 3D Inversion results

We now consider the 3D inversion results for the main study area identified in Fig. 1. Many inversion models were obtained. The final model results presented here employ a crustal scale length of 32 km with uniform voxels of $2 \times 2 \times 2$ km. The core area of the model contains $230 \times 500 \times 16$ voxel cells and is covered by 25,149 observations. The inversion uses an assumed 2nT data error floor and susceptibility amplitudes are unconstrained. The model chosen for presentation here uses distance weighting with smoothing across distance scales of $4 \times 4 \times 4$ km. The maximum value of susceptibility returned by the inversion, across the whole model, is 0.050 SI. It is worth noting that the voxel susceptibility values encompass a volume of 8 km^3 and may therefore differ from other sources (e.g. borehole) of information. The standard deviation of the model misfit is, once again, 2 nT. The form of the misfit obtained in the inversions is exemplified in Fig. 5.

3.1. A detailed example

The data conditioning (upward continuation) together with the voxel resolution of 2 km generates a simplified assessment of crustal magnetic structure. One advantage however is that the model is free from the often strong responses of at- and near-surface intrusive features such as dykes, plugs and sills. Here we first provide a brief, but more detailed, examination of the upper crustal model resolution using the Central Highland Grampian Terrane (CHGT). The Grampian phase of the Caledonian Orogeny records the collision of island arcs (the Midland Valley Terrane) with the margin of Laurentia during closure of the Iapetus Ocean in the early Palaeozoic (Lambert and McKerrow, 1976). Seven principal magmatic episodes extending from about 750 Ma to 390 Ma are outlined by Stephenson and Gould (1995). Here we make use of their numbering system for the Late-Tectonic and Post-Tectonic granites emplaced across the CHGT.

Fig. 10 shows the susceptibility distributions obtained for individual depth slices at (a) 2 km and (b) 8 km. The plots are overlaid with white polygons (with cross-hatch infill) defining (i) granite and (ii) lava outcrop mapping (at 1:250 k scale). The former group are contained entirely to the north of the Highland Boundary Fault (HBF) while the latter are contained to the south of the HBF (with the exception of lavas associated with the Blairgowrie (BL) anomaly). Granites numbered 46,

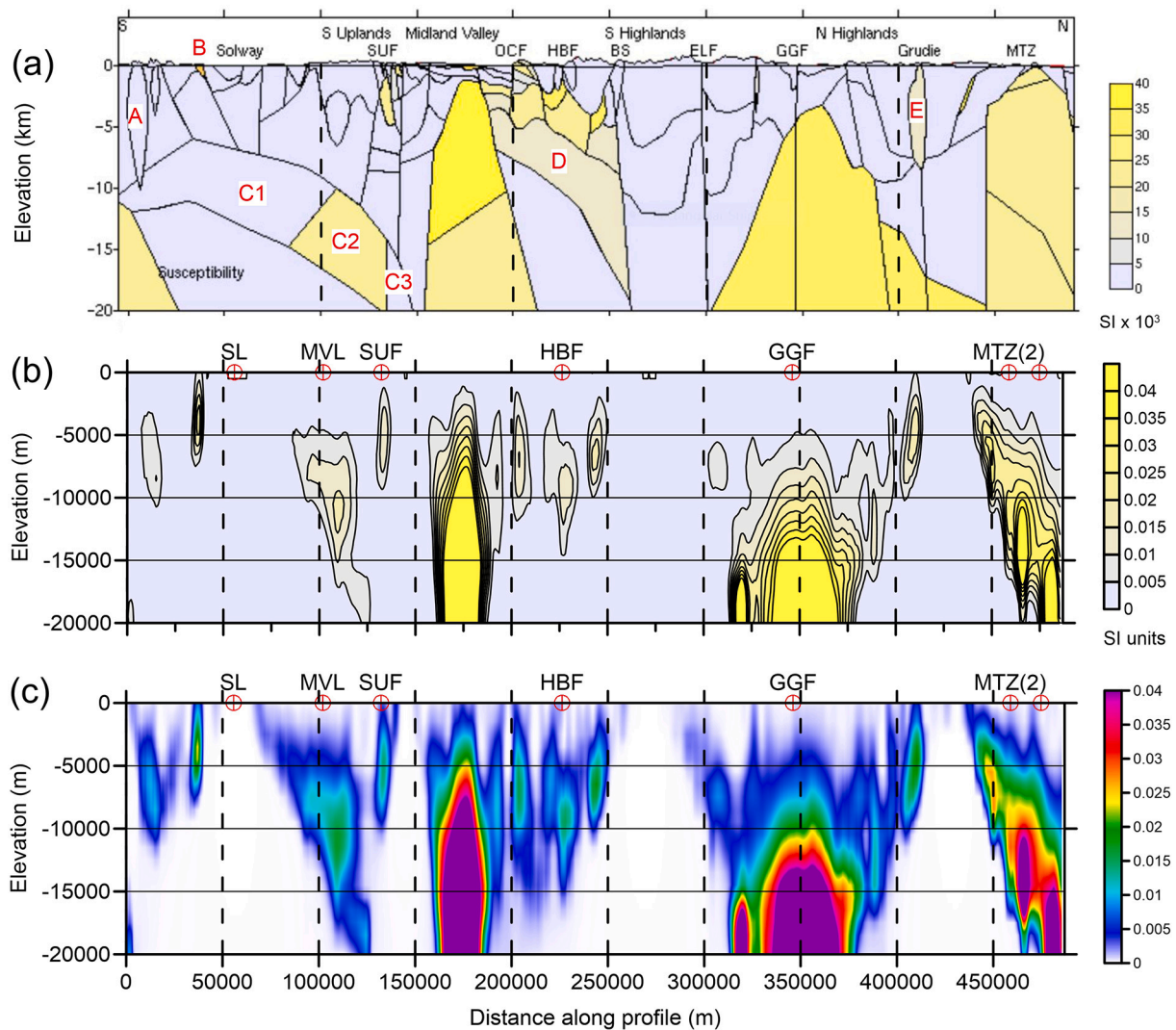


Fig. 9. Comparison of published and 3D inversion results along Northern Britain profile P27. (a) Published 2.5D inversion from Fig. 6. Red labels (A-E) discussed in text. (b) 3D inversion result shown using the same colour scale and contour interval as in (a). (c) 3D inversion result using continuous colour scale with same low/high range as in (a) and (b). Cross-hair symbols with labels denote location of terrane boundaries (Fig. 1 and Table 1) along the profile. Additional boundaries are MVL: Moffat Valley Lineament and SL: Solway Line. (For interpretation of the references to colour in this figure legend, the reader is referred to the web version of this article.)

47 and 51 are late tectonic, biotite-muscovite, intrusions and are non-magnetic. Intrusion 47 (Moy granite) was later intruded by a post tectonic magnetic granite (Saddle Hill granite) and this can perhaps be inferred by the horseshoe form of the anomaly at a depth of 2 km. The Post Tectonic Glen Tilt granite (GT) is also identified since it is spatially isolated and forms a simple vertical cylinder extending to a depth of about 8 km. This depth is consistent with the 9 km depth estimated by Rollin (2009) using 2.5D gravity modelling.

Both results in Fig. 10 identify the concealed roots of the granites with some individual centres amalgamating into larger zones with higher susceptibility by a depth of 8 km. An intriguing series of parallel intrusions following the Caledonian trend can be noted on the western margin of the area to the south of the GGF (red arrows in Fig. 10a) within the area mapped at the surface as the Rannoch Granite. Two additional anomalies are labelled RM (Rosemarkie) and BL (Blairgowrie). The Rosemarkie Inlier is a small fault-bounded lens of interleaved Moinian and Lewisian rocks with distinctive leucogranite (magnetic) veins and pods adjacent to the Great Glen Fault (GGF). The inlier is described in detail by Mendum and Noble (2010). The large Blairgowrie magnetic anomaly was modelled by Farquharson and Thompson (1992) using a detailed ground traverse. The main long wavelength anomaly in their

data was modelled as a deep (2 to 13 km) body with vertical magnetisation and an ultrabasic body was suggested. To the south of the Highland Boundary Fault concealed bodies with modest susceptibility are observed in association with the outcropping Devonian lavas.

One further feature is worth noting and that is the regional magnetic ridge, with no associated geological expression, arrowed and traced (heavy dotted black line) in Figs. 10 a,b. The trace, about 17 km to the NW of the Highland Boundary Fault (where parallel), abuts the Blairgowrie body in the east. Rollin (2009) suggested that the Midland Valley Terrane may extend beneath the CHGT for about 20 km north of the surface trace of the Highland Boundary Fault. The deeper model results and their implications are discussed later.

3.2. The 3D crustal model of Britain

The 3D crustal scale model is difficult to summarise since we have to extract 2D information in order to compare it with existing information. Rather than present the 16 horizontal slices through the 3D model, we simplify by averaging (arithmetic mean) the model across the 3 main depth scales of upper crust (0–10 km), middle crust (10–20 km) and lower crust (20–30 km). Although vertical resolution is reduced, the

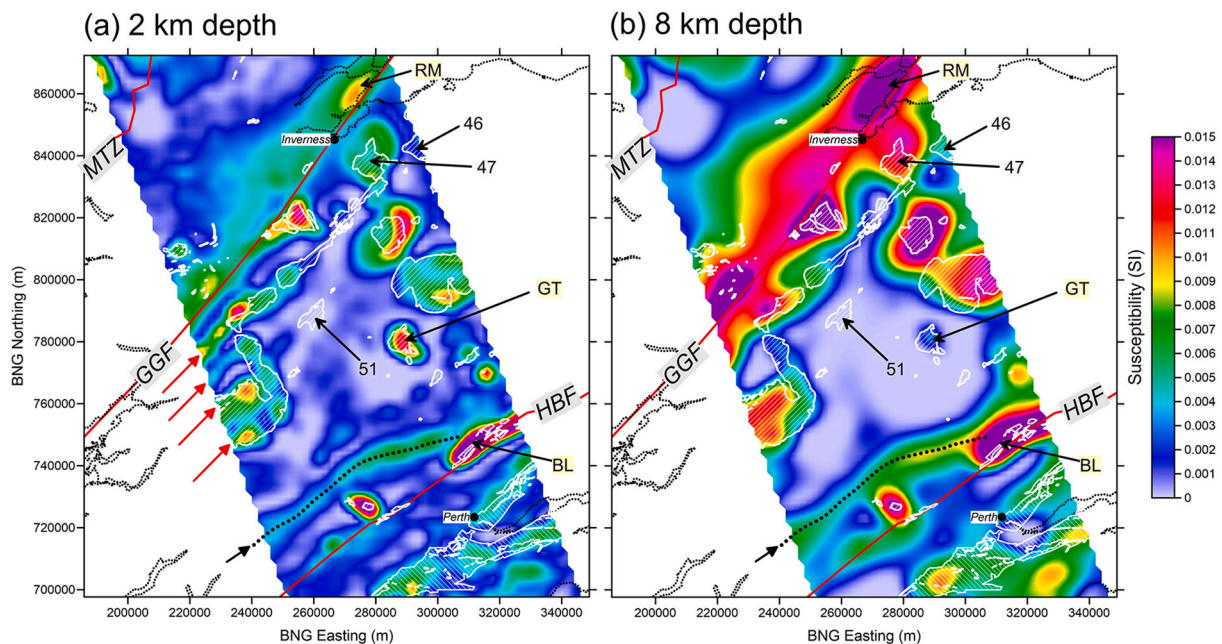


Fig. 10. Two upper crustal horizontal depth slices from 3D inversion of main study area centred on the Central Highlands Grampian Terrane (CHGT). (a) 2 km depth and (b) 8 km depth. White polygons with cross-hatch denote (i) granite outcrop (cross-hatch at 45°) and (ii) lavas (cross-hatch at -45°). Numbered granites are 46 (Ardclach), 47 (Moy), 51 (Strathspey). GT is Glen Tilt granite. RM is Rosemarkie Inlier magnetic anomaly. BL is Blairgowrie magnetic anomaly. Red lines are MTZ (Moine Thrust), GGF (Great Glen Fault), HBF (Highland Boundary Fault). Arrowed heavy dotted line is a feature discussed in the text. Coast is thin dotted black line. (For interpretation of the references to colour in this figure legend, the reader is referred to the web version of this article.)

averages reinforce the features which persist within the 3 depth intervals. The results are displayed in Figs. 11 a,b,c using a linear susceptibility scale. In order to maintain dynamic range the image for the upper crust is displayed using a reduced (x2) amplitude maximum. Each image shows the central profile P01 that is chosen to present an example of the crustal susceptibility cross-section across the model. It should be evident that the chosen cross section samples different features of the data (Fig. 1b) and 3D model (Fig. 11); for example the profile does not sample either of the two main anomalies in the vicinity of the Moine Thrust Zone (MTZ). The cross sectional information should therefore be viewed in tandem with these maps. We have chosen to present the cross-section in true scale using interval lengths of 250 km as shown in Fig. 12. The vertical resolution (2 km voxels) is low and the model is inherently smooth. In order to extract more structurally relevant information we can examine the spatial gradients across the model susceptibilities. As noted previously, we use the total (3D) spatial gradient (e.g. Lelièvre et al., 2009) across the model using Eq. (1). The 3D gradient is shown in Fig. 13 and at the lowest gradient amplitudes a level of noise is apparent.

4. Discussion

The model information presented in Figs. 11, 12 and 13 forms a crustal scale assessment of magnetic features across Britain with its associated terrane assemblage that have been studied and reported on for many decades. The study area is covered by 3 overlapping regional geophysical guides for South East England, Southern Scotland & Northern England and Northern Scotland (Busby et al., 2006; Kimbell et al., 2006; Rollin, 2009, respectively). The guides use the same aeromagnetic data set as here but also land-based gravity data and a wealth of geological and other relevant geoscientific information. To a large extent the studies provide modelling, interpretations and discussions of the magnetic features encountered in our 3D model. Here we note the more significant 3D features which, by virtue of a continuous and crustal-scale assessment, provide additional structural insights.

The most significant aspect of the model is the projection of upper crustal features and knowledge to deeper crustal levels. It is apparent in

Fig. 11 that the multitude of complex, high wavenumber, upper crustal structures are not resolvable by mid crustal depths but are still often associated with more extensive deeper magnetic roots. The deeper, more extensive features invariably possess higher susceptibilities, as exemplified in Fig. 10. By lower crustal depths, an assemblage of highly magnetic zones are separated by large volume non-magnetic areas.

4.1. Magnetic structure across northern (Laurentian) Britain

In the northern Laurentian terranes, the deeper crust (>10 km) encountered across the Hebridean Terrane (HT) and the Central Highlands Grampian Terrane (CHGT) is largely non-magnetic. Across the whole assemblage of British terranes, the susceptibility gradient to the SE of the Great Glen Fault (GGF, Fig. 12) forms the most intense crustal scale boundary. In contrast to published models, the concealed magnetic structure is asymmetric about the surface trace of the fault. The main upper crustal contribution is located to the SE of the fault with a deeper crustal inflection located beneath the fault itself. The degree to which the deeper magnetic basement is continuous across the fault zone and the implications in terms of defining a 'true' terrane boundary are discussed by Rollin (2009).

The magnetic ridge/edge observed some 17–20 km to the NW of the Highland Boundary Fault (HBF) is an upper crustal (<15 km) feature with the deeper crust being non-magnetic. The cross sections (Figs. 12 and 13) reveal a sequence of moderately magnetic zones (<0.020 SI) apparently connected by lower amplitude magnetic material sited above a basal ramp descending to the middle crust. We can also examine the HBF magnetic structure using the higher resolution (1 km voxels) 3D model previously shown in Fig. 9. The 3D inversion models the very clear sequential set of responses in the vicinity of the HBF (Fig. 7b) to an accuracy of ± 2 nT (Fig. 8). The profile location/azimuth used here (P27) differs from P01 as indicated in Fig. 7a. A 225 km true scale cross section (to a depth of 32 km) from the Solway Line in the south, through the Southern Upland and Midland Valley Terranes and into the CHGT in the north is displayed in Fig. 14. Both the susceptibility and spatial gradient of the susceptibility are shown. The resolution along profile

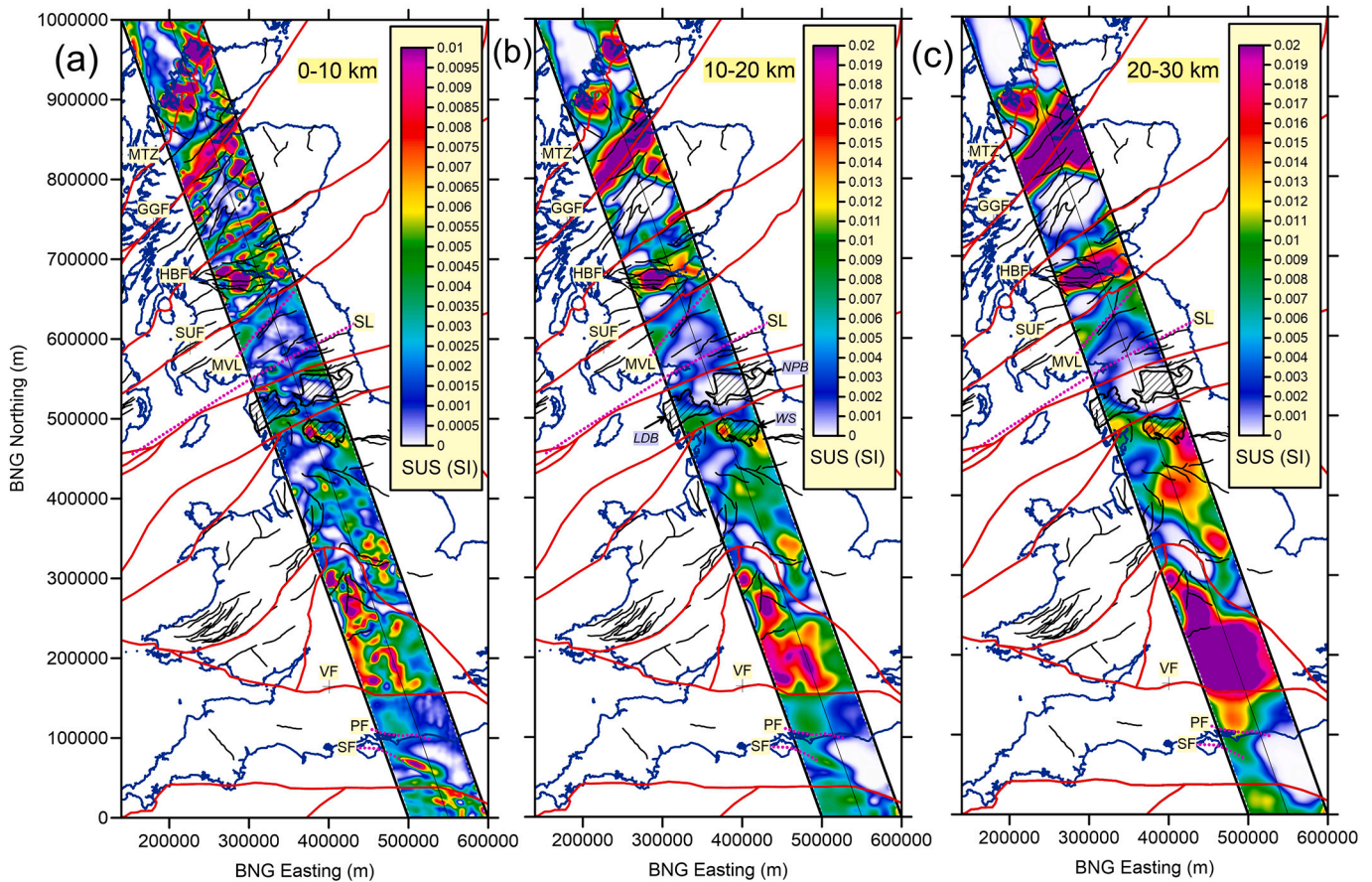


Fig. 11. 3D inversion results of vertical arithmetic averages of susceptibility within 3 depth ranges (a) 0–10 km. (b) 10–20 km and (c) 20–30 km. The amplitude range of (a) is reduced by a factor of 2. Labels denote location of terrane boundaries (Fig. 1 and Table 1). Additional boundaries are MVL: Moffat Valley Lineament, SL: Solway Line, VF: Variscan Front, PF: Portsdown-Middleton Fault and SF: Sandown Fault. Centre line of data polygon is profile P01. Black lines across whole onshore area denote mapped faults (1:625 k) > 30 km in length. Two polygons (with cross-hatch) in Leinster-Lakesman Terrane (LLT) denote granite batholiths at a modelled depth of 8 km, LDB (Lake District Batholith) and concealed NPB (North Pennine Batholith). A third polygon to the south of terrane boundary within the Caledonides of Southern Britain (CSB) is the concealed Wensleydale Granite (WS) at a modelled depth of 3 km. Depths from 3D gravity models of Kimbell et al. (2006).

P27 is significantly enhanced and the three main bodies straddling the HBF are more compact than their lower resolution counterparts along profile P01.

If we define the MVT in terms of the presence of magnetic igneous basement material (an assumed assemblage of volcanic arcs and/or Ballantrae-like ophiolitic material) and the CHGT basement as being non-magnetic then the observed magnetic structures are significant. The observation is consistent with previous discussions/speculations by Bluck (1984) and Dentith et al. (1992) and distilled by Rollin (2009) who all indicated that the Midland Valley Terrane may extend beneath the CHGT for about 20 km north of the surface trace of the Highland Boundary Fault. It is also worth noting the final deep seismic velocity model obtained by the LISPB refraction experiment (Barton, 1992). The LISPB profile crosses the HBF some 21.5 km to the NE of profile P01. Barton (1992) notes that between 20 km to the north of the HBF and the HBF itself there is a shallow zone of lower velocity between depths of about 2 and 4 km. Beneath this zone there is a strong southward increase in velocities between depths of 4 to 20 km and therefore the concealed magnetic zone may define the final docking position of the Midland Valley. The upper crustal structures associated with the main Bathgate anomaly, central to the MVT, are connected to a deep crustal, high susceptibility zone in the lower crust. The zone, some 25 km in width, is second only to the GGF in volumetric crustal extent (Fig. 11).

The main anomaly associated with the central section of the SUF is limited in lateral extent (40 km) and straddles the fault (Fig. 7). The

cross-sections (Figs. 12 and 14) indicate it is an isolated upper crustal feature interpreted by Kimbell et al. (2006) as a potential ophiolite. In Fig. 12, to the south of the SUF the SUT displays moderate susceptibilities as far south as the MVL. The main anomaly is located in the middle crust and is largely concealed. As previously noted, the higher resolution cross-section along P27 (Fig. 14) images a northward dipping feature in the upper and middle crust (<20 km). The distinct geometry of the feature, dipping north at an angle of 15°, however is not observed along profile P01. The 2 profiles sample 2 distinct low amplitude magnetic features straddling the Moffat Valley Lineament (MVL) as shown in Fig. 7. The lack of any significant magnetic response across the projected closure zone of Iapetus is well documented (within the central swathe discussed here). Kimbell and Stone (1995) and Kimbell et al. (2006) review the geophysical evidence and discuss the competing hypotheses relating to the geometry of accretion and final closure. Given the results obtained here, a higher resolution 3D assessment of the whole Southern Upland Terrane appears warranted. In Fig. 12, to the SE of the MVL only very low, or zero, susceptibilities are encountered until a slight change in character is observed at the terrane boundary with the LLT.

4.2. Magnetic structure across southern (Avalonian) Britain

The Avalonian terranes to the south of the Solway Line are now considered. Here the ‘Caledonian’ basement is largely concealed by later strata and potential field data have long been used to identify some of

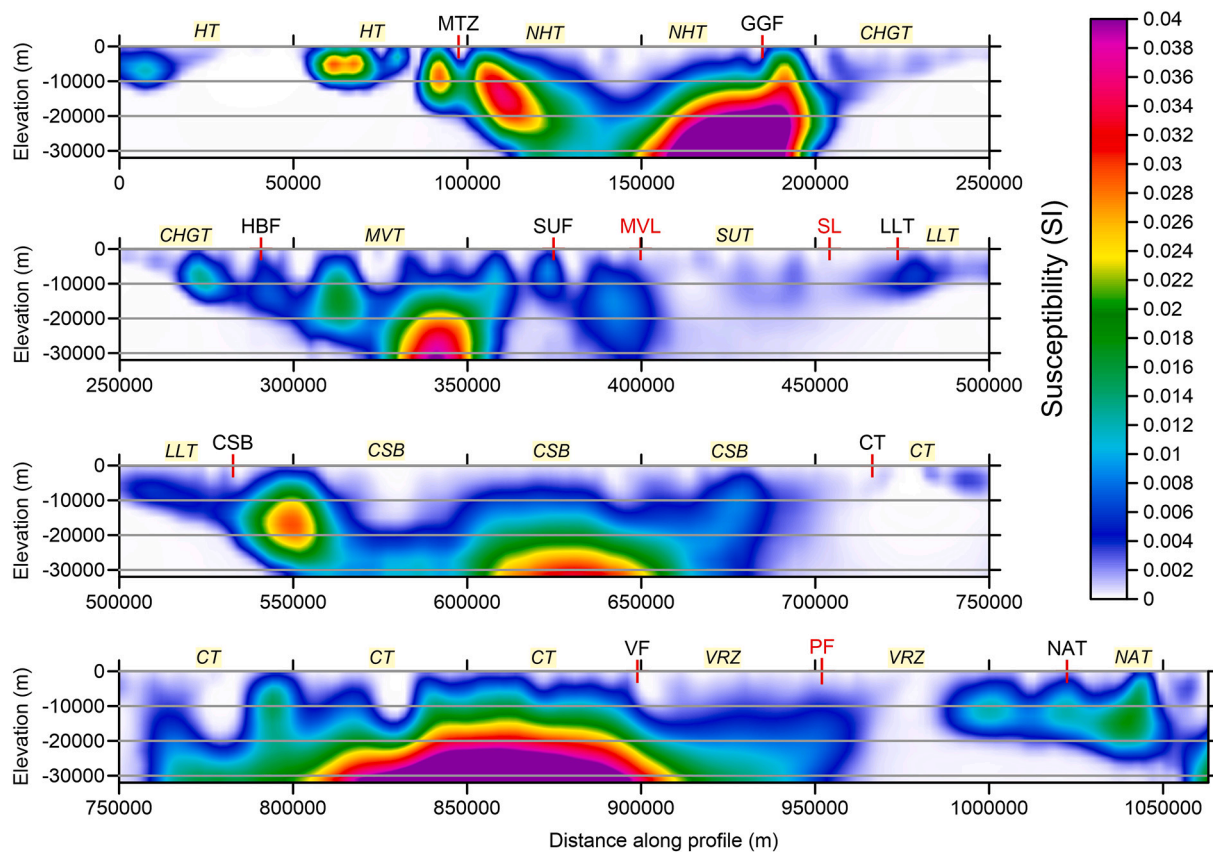


Fig. 12. 3D inversion susceptibility results as a cross-section along profile P01 plotted in true scale using initial sub-section lengths of 250 km. The profile runs from North to South. Labels denote location of terranes and terrane boundaries (Fig. 1 and Table 1). Additional boundaries are MVL: Moffat Valley Lineament, SL: Solway Line, PF: Portsdown/Middleton Fault.

the broad structural trends (Lee et al., 1990). A series of suspected magnetic volcanic arc complexes extend southwards into the Charnwood Terrane. They are considered to result from subduction of oceanic lithosphere beneath Avalonia prior to collision with Baltica and Laurentia in late Ordovician and Silurian time, respectively (Pharaoh et al., 1995).

The Leinster-Lakesman Terrane (LLT) study area contains 2 large intrusive sequences namely the Lake District Batholith (partially exposed) and the concealed North Pennine Batholith (containing the Weardale granite). Kimbell et al. (2006) indicate the two plutons were formed in the footwall of the Iapetus Suture. The outlines of the batholiths at a depth of ~ 8 km obtained from 3D gravity modelling (Kimbell et al., 2006; Kimbell et al., 2010) are shown in Fig. 11. Additionally, the concealed and thinner Wensleydale granite, within the Caledonides of Southern Britain (CSB) Terrane, is outlined at a modelled depth of 3 km. The 3D forms of the modelled density contrasts are given in detail by Kimbell et al. (2006). Referring now to the magnetic features across the terrane, we note that in the upper crust (Fig. 11a) the various granites/granodiorite across the Lake District Batholith appear only slightly magnetic (susceptibilities < 0.002 SI). The Shap granite (in the SE corner) is a clear exception. The Weardale granite is non-magnetic and gravity studies, following the early work of Bott (1967), indicate a single low density mass with 5 cupolas (Kimbell et al., 2010). These authors indicate there is evidence of magnetised basement rocks or denser magnetic intrusive phases on the flanks of the non-magnetic, low density plutons. It was suggested that the long-wavelength magnetic null could be explained in part by the granite puncturing a deeper magnetic basement, and generating a demagnetized zone below the granite to depths of 16–20 km. The 3D model (Fig. 11) indicates however that a non-magnetic basement occupies the whole crust below a depth of about

10 km.

A semi-continuous belt of magnetic material is observed abutting the southern margin of the Lake District Batholith (in the upper crust) and then trending ESE across the CSB terrane. Bott (1967) noted that the then postulated Wensleydale granite punctured the magnetic belt. The form of the puncture can be seen in Fig. 11a. The magnetic belt can be traced from the location shown as far as East Anglia and was referred to as the Furness-Norfolk anomaly by Beamish et al. (2016). Pharaoh (2018) reprising the geophysical information summarises several decades of speculation as to the cause of the magnetic features largely confined to the upper crust. Fig. 11 demonstrates that the belt, although of variable magnetisation, occupies a whole crustal interval. In the deeper crust (> 20 km) the magnetic belt underlies the LDB. Profile P01 traverses the magnetic belt in the vicinity of a local magnetic high within the Wensleydale granite. Figs. 12 and 13 image this feature with a northern edge at the Terrane boundary and the main magnetic high centred in the middle crust and with a component of southerly dip within the lower crust. The LLT terrane in cross-section is characterised by low susceptibilities (< 0.004 SI) occupying the upper crust which descend to the middle crust in the south in the vicinity the terrane boundary with the CSB.

Within the CSB terrane lies a second belt of magnetic features which are discontinuous in the upper crust but overlie a continuous magnetic belt at progressively deeper levels. This NW trending zone is referred to as the Derby-St. Ives anomaly (Pharaoh, 2018). The zone appears to terminate at the terrane boundary with the Charnwood Terrane at deeper crustal levels (Fig. 11b). In cross section, the CSB terrane is characterised by high susceptibilities in the lower crust but the location of profile P01 limits an adequate sampling of the entire belt. According to Beamish et al. (2016), the magnetic trends observed in the two

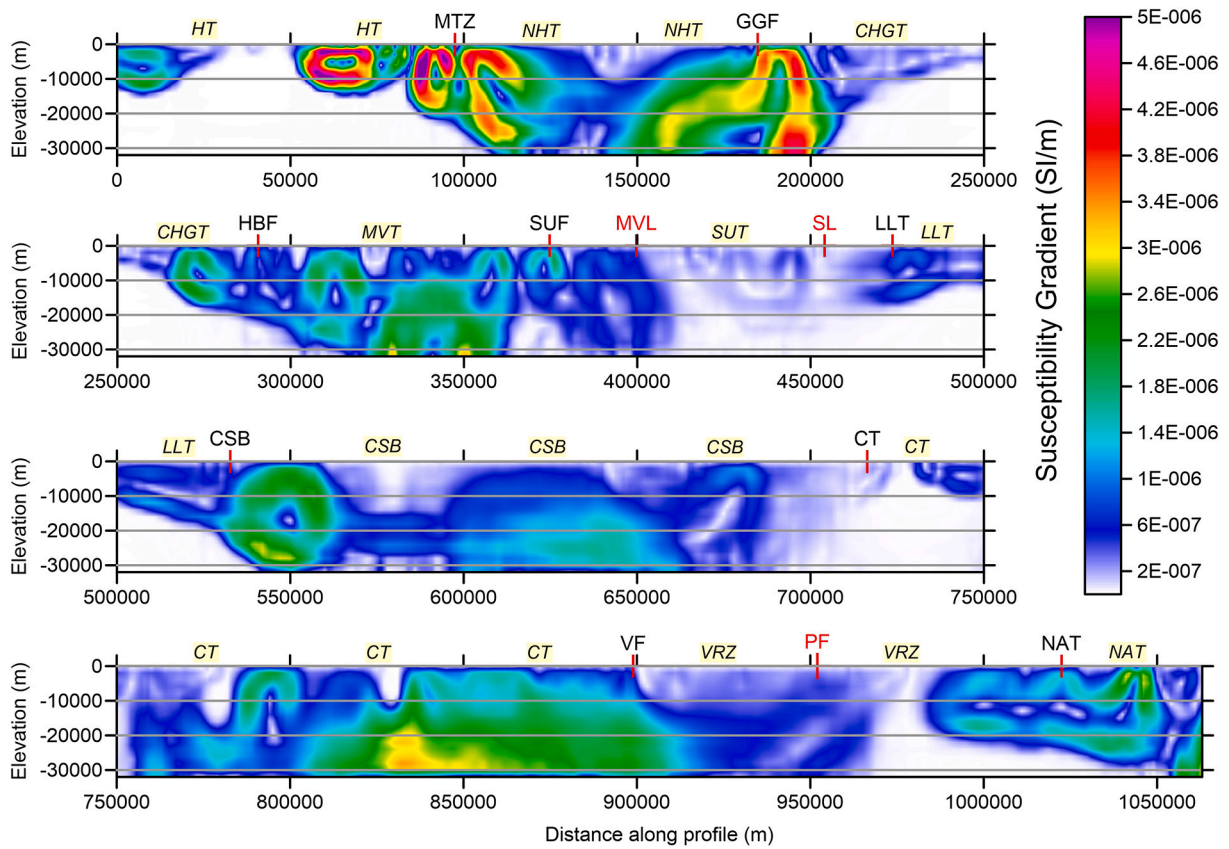


Fig. 13. 3D inversion total gradient of susceptibility (Fig. 12) as a cross-section along profile P01 plotted in true scale using initial sub-section lengths of 250 km. The profile runs from North to South. Labels denote location of terranes and terrane boundaries (Fig. 1 and Table 1). Additional boundaries are MVL: Moffat Valley Lineament, SL: Solway Line, PF: Portsdown/Middleton Fault.

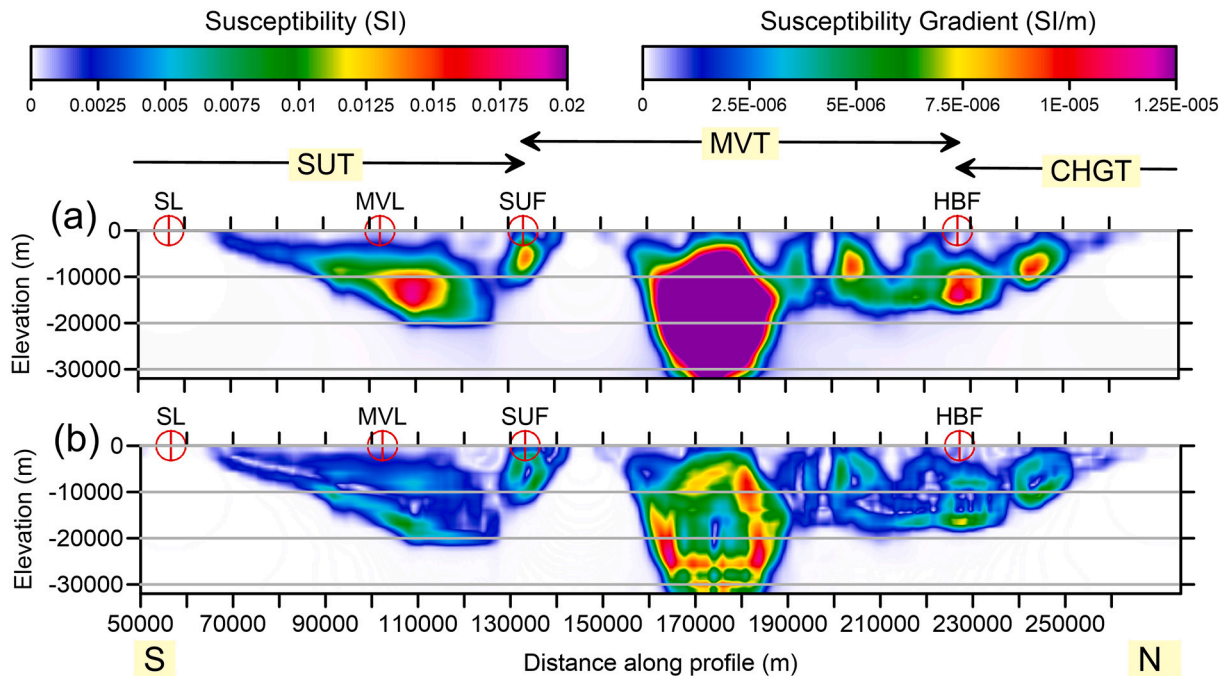


Fig. 14. Detail of 3D inversion of results along a cross-section of the Northern Britain profile P27 (see Fig. 9) plotted in true scale. Profile takes in northern portion of Southern Uplands Terrane (SUT), the Midland Valley Terrane (MVT) and southern portion of Central Highland Grampian Terrane (CHGT). (a) Susceptibility and (b) total gradient of susceptibility. Boundaries shown are SL (Solway Line), MVL (Midland Valley Lineament), SUF (Southern Uplands Fault) and HBF (Highland Boundary Fault).

regional-scale belts suggest a cause involving the products of Ordovician arc magmatism associated with the south-westward subduction of the Tornquist Ocean (Pharaoh et al., 1993).

The Charnwood Terrane is characterised by the highest lower crustal susceptibilities observed across all of the Avalonian Terranes. The complex sequence of upper crustal anomalies amalgamate at depth into a high susceptibility zone in the deeper crust. Susceptibilities in the large central zone increase from 0.035 to 0.06 SI in the lower crust. This Precambrian basement is part of Avalonian basement of the Midlands Microcraton and may represent the oldest basement fragment in the area. The high susceptibilities are ascribed to silicic volcanic and volcanoclastic rocks, inferred in the upper crust, being replaced by more intermediate, magnetite-rich plutonic magmatic rocks with increasing depth (Pharaoh, 2018). The Variscan Front in the south provides a clear demarcation of the magnetic structures associated with the Charnwood Terrane. Additionally a southward extension is observed at middle and lower crustal depths largely to the west of profile P01. The imaging of this feature confirms previous modelling and assessments by Busby and Smith (2001) and Busby et al. (2006) which indicated the burial of magnetic basement beneath less magnetic rocks caused by northward-verging Variscan thrusts. This deeper magnetic spur extends as far south as the Portland-Middleton Fault (PF). The tectonic significance of this thrust fault is discussed by Busby and Smith (2001). To the south of the Portland-Middleton fault (PF), a significant linear, upper to middle, crustal anomaly is associated with the Sandown Fault (SF) which to the SE becomes the Pays de Bray Fault. The magnetic structure is limited in extent and terminates in an extensive zone of non-magnetic crust. Further south two upper crustal magnetic features appear firstly in association with the boundary of the Variscide Internide Zone (VRZ) and North Armorican Composite Terrane (NAT). The cross-sections of Figs. 12 and 13 provide a useful summary of the structures encountered. The two southernmost structures may connect at depth to the Sandown Fault structure to the north. All three occupy an upper to middle crustal volume and display a remarkably similar corrugated form.

5. Conclusions

The present study has demonstrated the application of regularised 3D magnetic inversion methods to a large scale, but low resolution, aeromagnetic data set across Britain. We have established how this can be achieved at the crustal scale using voxel scales of both 1 and 2 km and only modest computer resources. The Curie isotherm depth, rather than the seismic/petrological Moho depth, forms the base of the all the crustal magnetic models considered. An investigation of the effects of assigning different crustal magnetic depths in the inversion procedure was carried out. It was found that adequate model misfits could be obtained using model depth assignments of between 5 and 40 km. Given this intrinsic algorithmic behaviour it was noted that the Curie depth is better supplied as an independent constraint. This is available as a global model, with a spatial resolution of about 50 km, from the work of Li et al. (2017). Across onshore Britain we note the recent higher resolution (~11 km) Curie depth model of Baykiev et al. (2018). It is possible, in more complex situations, to apply a spatially non-uniform base to the 3D model discretisation. A crucial aspect of the 3D inversion of potential fields is the incorporation of depth, or distance, weighting. Here we provide a crustal scale example of the models obtained by the 2 approaches. Fig. 3 summarises the model variability that can be expected. Both approaches return approximately the same lateral configuration of enhanced susceptibilities but the precise values differ. The depth weighting solution provides some higher value zones than its distance weighting counterpart and, as might be expected, the former solution may provide more 'vertically compact' behaviour. We have compared our 3D inversion results with an existing geologically-constrained 2.5D profile inversion across northern Britain. The predicted data of the 3D inversion fit the observations with a high degree of fidelity at all wavelengths. The comparison conducted indicates that if the 2.5D

model is considered geologically/tectonically plausible then the 3D model should be considered equally plausible and more accurate. The 3D susceptibility models were not excessively noise-prone (when assessed using their spatial gradients) but can benefit from modest levels of smoothing. Such smoothing can be carried out using the control parameters of the MAG3D inversion or by subsequent 3D filtering (smoothing) within the voxel volume.

The 3D magnetic model of Britain was obtained using 2 km scale voxels. In order to summarise what is a coarse crustal assessment we have employed susceptibility averages obtained across the upper, middle and lower crust depth intervals. The provision of a representative crustal scale cross-section, over 1000 km in length, and traversing 10 of the main British terranes, is perhaps the most valuable feature of the inversion model. The associated presentation of the model spatial gradients is also useful when comparing the levels of 'structural contrast' within the smooth model inversion assessment. A significant aspect of the model is the projection of upper crustal features to deeper crustal levels. Many localised upper crustal anomalies display deeper, increasingly magnetic, roots which by lower crustal depths form a terrane-based zonation of magnetic areas separated by large volume non-magnetic areas. Our discussion of the results obtained is set within a context of many decades, and indeed centuries, of geological studies of the British subsurface. The Glen Tilt granite (Fig. 10) was an evidential location visited in 1785 by Hutton when forming his theory of 'Plutonism' (Hutton, 1794). Here we provide only a brief discussion of the more significant model features relating to the extensive literature. Finally we note that the use of a 'reduced width' swathe of data has proven largely adequate and indicates that similar crustal assessments could be undertaken using many existing country-wide aeromagnetic data sets while employing only modest computer resources.

Data availability

The study used a data subset of the baseline aeromagnetic survey of Britain which is available from <https://www.bgs.ac.uk/products/geophysics/aeromagneticRegional.html>.

Author contributions

DB initiated the project and performed the geophysical analysis. TCP undertook the geological/tectonic analysis. DIS supported the writing, review and editing.

Declaration of Competing Interest

None.

Acknowledgements

We thank Jon Busby for internal reviews. This research did not receive any specific grant from funding agencies in the public, commercial or not-for-profit sectors. This paper is published with the permission of the Executive Director, British Geological Survey (NERC).

Appendix A. Supplementary data

Supplementary data to this article can be found online at <https://doi.org/10.1016/j.tecto.2021.228982>.

References

- Andersson, M., Malehmir, A., 2018. Internal architecture of the Alnö alkaline and carbonatite complex (Central Sweden) revealed using 3D models of gravity and magnetic data. *Tectonophysics* 740-741, 53–71. <https://doi.org/10.1016/j.tecto.2018.05.008>.
- Barton, P.J., 1992. LISPB revisited: a new look under the Caledonides of northern Britain. *Geophys. J. Int.* 110, 371–391.

- Baykiev, E., Guerri, M., Fullea, J., 2018. Integrating Gravity and Surface Elevation with magnetic Data: Mapping the Curie Temperature beneath the British Isles and Surrounding areas. *Front. Earth Sci.* 6, 165. <https://doi.org/10.3389/feart.2018.00165>.
- Beamish, D., Kimbell, G.S., Pharaoh, T., 2016. The deep crustal magnetic structure of Britain. *Proc. Geol. Assoc.* 127 (6), 647–663. <https://doi.org/10.1016/j.pgeola.2016.10.007>.
- Bluck, B.J., 1984. Pre-Carboniferous history of the Midland Valley of Scotland. *Trans. R. Soc. Edinb. Earth Sci.* 75, 275–295.
- Bluck, B.J., Gibbons, W., Ingham, J.K., 1992. Terranes. In: Cope, J.C.W., Ingham, J.K., Rawson, P.F. (Eds.), *Atlas of Palaeogeography and Lithofacies*, 13, pp. 1–4. *Journal of the Geological Society, London, Memoirs*.
- Bott, M.H.P., 1967. Geophysical investigations of the northern Pennine basement rocks. *Proc. Yorks. Geol. Soc.* 36, 139–168.
- Busby, J.P., Smith, N.J.P., 2001. The nature of the Variscan basement in Southeast England: evidence from integrated potential field modelling. *Geol. Mag.* 138 (6), 669–685. <https://doi.org/10.1017/S0016756801005751>.
- Busby, J.P., Walker, A.S.D., Rollin, K.E., 2006. *Regional Geophysics of South-East England. Version 1.0*. On CD-ROM. British Geological Survey, Keyworth, Nottingham.
- Cocks, L.R.M., Fortey, R.A., 1982. Faunal evidence for oceanic separations in the Palaeozoic of Britain. *J. Geol. Soc. Lond.* 139, 465–478.
- Cocks, L.R.M., McKerrow, W.S., Van Staal, C.R., 1997. The margins of Avalonia. *Geol. Mag.* 134, 627–636.
- Dentith, M.C., Trench, A., Bluck, B.J., 1992. Geophysical constraints on the nature of the Highland Boundary Fault Zone in Western Scotland. *Geol. Mag.* 129, 411–419.
- Dewey, J.D., Strachan, R.A., 2003. Changing Silurian-Devonian relative plate motion in the Caledonides: sinistral transpression to sinistral transtension. *J. Geol. Soc. Lond.* 160, 219–229.
- Farquharson, C.G., Thompson, R., 1992. The Blairgowrie magnetic anomaly and its interpretation using simple optimisation. *Trans. R. Soc. Edinb. Earth Sci.* 83, 509–518.
- Frost, B.R., Shive, P.N., 1986. Magnetic mineralogy of the lower continental crust. *J. Geophys. Res.* 91, 6513–6521.
- Goodwin, J.A., Hackney, R., Williams, N.C., 2015. 3D Geophysical inversion modelling of the Wallaby Plateau: evidence for continental crust and seaward-dipping reflectors. In: *Record 2015/01*. Geoscience Australia, Canberra. <https://doi.org/10.11636/Record.2015.001>.
- Hutton, J., 1794. Observations on granite. *Earth Environ. Sci. Trans. Royal Soc. Edinburgh* 3, 77–85.
- Kimbell, G.S., Stone, P., 1995. Crustal magnetization variations across the Iapetus Suture Zone. *Geol. Mag.* 132, 599–609.
- Kimbell, G.S., Carruthers, R.M., Walker, A.S.D., Williamson, J.P., 2006. Regional geophysics of southern Scotland and Northern England. In: *Version 1.0 on CD-ROM*. British Geological Survey, Keyworth, Nottingham.
- Kimbell, G.S., Young, B., Millward, D., Crowley, Q.G., 2010. The North Pennine batholith (Weardale Granite) of northern England: new data on its age and form. *Proc. Yorks. Geol. Soc.* 58 (2), 107–128. <https://doi.org/10.1144/pygs.58.1.273>.
- Lambert, R.S.J., McKerrow, W.S., 1976. The Grampian Orogeny. *Scott. J. Geol.* 12, 271–292.
- Lee, M.K., Pharaoh, T.C., Soper, N.J., 1990. Structural trends in Central Britain from images of gravity and aeromagnetic fields. *J. Geol. Soc.* 147, 241–258.
- Lelièvre, P.G., Oldenburg, D.W., Williams, N.C., 2009. Integrating geological and geophysical data through advanced constrained inversions. *Explor. Geophys.* 40 (4), 334–341. <https://doi.org/10.1071/EG09012>.
- Li, C.-F., Lu, U., Wang, J., 2017. A global reference model of Curie-point depths based on EMAG2. *Nat. Sci. Rep.* 7, 45129. <https://doi.org/10.1038/srep45129>.
- Li, Y., Oldenburg, D.W., 1996. 3-D inversion of magnetic data. *Geophysics* 61, 394–408.
- McKerrow, W.S., Dewey, J.F., Scotese, C.R., 1991. The Ordovician and Silurian development of the Iapetus Ocean. In: Bassett, M.G., Lane, P.D., Edwards, D. (Eds.), *The Murchison Symposium*, 42. *Spec. Papers in Palaeontology*, pp. 165–176.
- Mendum, J.R., Noble, S.R., 2010. Mid-Devonian sinistral transpression on the Great Glen Fault: the rise of the Rosemarkie Inlier and the Acadian Event in Scotland. In: Law, R. D., Butler, R.W.H., Holdsworth, R.E., Krabbendam, M., Strachan, R.A. (Eds.), *Continental Tectonics and Mountain Building: The Legacy of Peach and Horne*, 335. Geological Society, London, Special Publication, pp. 161–187.
- Pharaoh, T., 2018. The Anglo-Brabant Massif: persistent but enigmatic palaeo-relief at the heart of western Europe. *Proc. Geol. Assoc.* 129 (3), 278–328. <https://doi.org/10.1016/j.pgeola.2018.02.009>.
- Pharaoh, T.C., Carney, J., 2000. Introduction, chapter 1. In: Carney, J., Horak, J.M., Pharaoh, T.C., Gibbons, W., Wilson, D., Barclay, B.J., Ford, T.D. (Eds.), *Precambrian rocks of England and Wales*. Geological Conservation Review, Joint Nature Conservation Committee-Chapman & Hall, pp. 1–18, 239pp.
- Pharaoh, T.C., Brewer, T.S., Webb, P.C., 1993. Subduction-related magmatism of late Ordovician age in eastern England. *Geol. Mag.* 130, 647–656.
- Pharaoh, T.C., England, R., Lee, M., 1995. The concealed Caledonide basement of Eastern England and the southern North Sea - a review. *Stud. Geophys. Geod.* 39, 330–346.
- Pharaoh, T.C., Morris, J., Long, C.B., Ryan, P.D., 1996. *The Tectonic Map of Britain, Ireland and adjacent areas. Sheet 1. 1:1 500 000 Scale*. Br. Geol. Surv. Geol. Surv. Ireland. ISBN 0751831298.
- Rollin, K.E., 2009. *Regional geophysics of Northern Scotland*. In: *Version 1.0 on CD-ROM*. British Geological Survey, Keyworth, Nottingham.
- Schofield, D.I., Leslie, A.G., Wilby, P.R., Dartnall, R., Waldron, J.W.F., Kendall, R.S., 2020. Tectonic evolution of Anglesey and adjacent mainland North Wales. In: Murphy, J.B., Strachan, R.A., Quesada, C. (Eds.), *Pannotia to Pangaea: Neoproterozoic and Paleozoic Orogenic Cycles in the Circum-Atlantic Region*, 503. Geological Society, London, Special Publications. <https://doi.org/10.1144/SP503-2020-9>.
- Soper, N.J., England, R.W., Snyder, D.B., Ryan, P.D., 1992. The Iapetus suture zone in England, Scotland and eastern Ireland: a reconciliation of geological and deep seismic data. *J. Geol. Soc. Lond.* 149, 697–700.
- Spicer, B., Morris, B., Ugalde, H., 2011. Structure of the Rambler Rhyolite, Baie Verte Peninsula, Newfoundland: Inversions using UBC-GIF Grav3D and Mag3D. *J. Appl. Geophys.* 75 (1), 9–18.
- Stephenson, D., Gould, D., 1995. *British Regional Geology: The Grampian Highlands*, Fourth edition. British Geological Survey, Keyworth, Nottingham. Reprint 2007.
- Stephenson, D., Mendum, J.R., Fettes, D.J., Smith, C.G., Gould, D.P., Tanner, P.W.G., Smith, R.A., 2013. The Dalradian rocks of the north-east Grampian Highlands of Scotland. *Proc. Geol. Assoc.* 124, 318–392.
- Stone, P., Green, P.M., Lintern, B.C., Simpson, P.R., Plant, J.A., 1993. Regional geochemical variation across the Iapetus Suture zone: tectonic implications. *Scott. J. Geol.* 29, 113–121.
- Trench, A., Torsvik, T.H., 1992. The closure of the Iapetus Ocean and Tornquist Sea: new palaeomagnetic constraints. *J. Geol. Soc. Lond.* 149, 867–870.
- Welford, J.K., Hall, J., 2007. Crustal structure of the Newfoundland rifted continental margin from constrained 3-D gravity inversion. *Geophys. J. Int.* 171, 890–908. <https://doi.org/10.1111/j.1365-246X.2007.03549.x>.
- Williams, N.C., 2008. *Geologically Constrained UBC-GIF Gravity and Magnetic Inversions with Examples from the Agnew-Wiluna Greenstone Belt, Western Australia*. PhD thesis. University of British Columbia, Vancouver, BC.